SPECTROSCOPIC PROPERTIES AND RESISTIVITIES OF

SOME ALKALI METAL-ARENE CHARGE-

TRANSFER COMPLEXES

By

PAUL CHING LI

Bachelor of Science

Taiwan Provincial Chung-hsing University

Taichung, Taiwan

Republic of China

1959

Submitted to the Faculty of the Graduate College
of the Oklahoma State University
in partial fulfillment of the requirements
for the Degree of
DOCTOR OF PHILOSOPHY
May, 1973

SPECTROSCOPIC PROPERTIES AND RESISTIVITIES OF

SOME ALKALI METAL-ARENE CHARGE-

TRANSFER COMPLEXES

Thesis Approved:

J Paul Devlin
Thesis Adviser

Herbert A. Pohl

N. Purdie

George Gorin

N. N. Durham
Dean of the Graduate College

ii

ACKNOWLEDGEMENTS

The author first of all wishes to express his deepest appreciation to Professor J. Paul Devlin, for his guidance, enthusiasm and encouragement throughout the course of this study, not to mention his invaluable assistance during the preparation of the manuscript of the thesis. He would like to thank Dr. E. J. Eisenbraun for the loan of the purest naphthalene and cyclohexane.

Gratitude is expressed to Dr. H. A. Pohl for his interest and partial financial support in this study of the semiconductive charge-transfer complexes.

Thanks to Messrs Hall and Adkins and their associates for their help in making the apparatus.

The author is indebted to his wife Kao-chi for her thoughtfulness and understanding during his graduate study at Oklahoma State University.

This study was made possible by financial support from the Oklahoma State Research Foundation through a National Science Foundation Grant.

TABLE OF CONTENTS

TABLE OF CONTENTS (Continued)

LIST OF TABLES

LIST OF FIGURES

CHAPTER I

INTRODUCTION

The Problem

The solid binary mixtures between alkali metals and polycyclic aro-
matic hydrocarbons formed via gas phase co-condensation (1) are con-
sidered, qualitatively, to be either donor-acceptor type charge transfer
(CT) complexes or solid solutions formed by the solvation of alkali
metal atoms into the interstices of the polycyclic aromatic hydrocarbon
crystals. The optical and electrical properties of these mixtures in the
form of thin solid films have not been reported. It was, therefore, of
interest to investigate these thin solid films experimentally and theo-
retically.

Characterization of these binary mixtures is necessary to an under-
standing of their structures as well as the semiconductive properties.
Particularly, these materials obtained from gas phase co-condensation are
expected to display some unusual electrical and optical effects. There-
fore, extensive spectroscopic work was dedicated to the characterization
tion of these mixtures. A deeper insight concerning the nature of con-
duction and energy level structure of these solids could be expected
from the optical and conductivity measurements.

The first part of this thesis deals with theoretical consideration
of the optical and electrical properties in terms of a charge-transfer
process. Chapter III will provide a description of the detailed experi-

1

mental methods for sample preparation, i.e., co-condensation, as well as techniques used in obtaining optical and electrical properties for mainly the potassium-naphthalene system. Results and possible interpretations will be presented in Chapter IV. Since this approach can be applied to a large number of chemical systems, proposed objectives for future study are also included in Chapter IV. Particular attention is devoted to the preparation of binary mixtures between alkali metals and polyarenes. Potassium has been selected for the electron donor, naphthalene is chosen for electron acceptor. The optical properties (ir, Raman, luminescent and visible absorption spectra) and electrical resistivities of the mixtures are the principle concerns of this investigation.

The Appendix, which has been published (2), presents some fairly conclusive results regarding the potassium-anthracene systems. For example, spectroscopic data obtained for a range of the metal-organic deposition ratios provides evidence for the existence of three stoichiometric salt-like crystalline solids, i.e., 2:1; 1:1 and 1:2 complexes. The vibrational data represent the best available empirical evidence of the effect of electron transfer on the bond strength in anthracene. Direct identification of these species in future work should now be possible. The Raman sampling technique used and the colored nature of the sample favored the observation of a strong resonance Raman effect with 5145 $\overset{o}{A}$ line (green) for scattering produced by the anthracene symmetric skeletal mode in the K_2A salt. The electronic absorption spectra in the visible region, obtained to compare with the solution data, supports the observation of the resonance Raman effect. Resistivities which were measured at about $100^{o}K$ using a four-point-probe technique should be valuable to compare with the data reported by Ubbelohde (13, 16).

Published reports concerning these systems are numerous (3-21), but most previous sample preparations were either in solution, solid complexes isolated after reaction in inert solvents, or layered complexes prepared by evaporation of one component onto a thin film of the second component. Only electronic fluorescent spectra for solid samples of unknown composition obtained from gas phase co-condensation of alkali metals with anthracene have been reported by Slobodyanik and Faidysk (11).

It is worth noting that these complexes are extremely reactive toward traces of moisture and oxygen; they have thus been prepared in an inert atmosphere, and have only been available in limited amounts. Furthermore, solutions of the anions of various arenes prepared in inert solvents (e.g., tetrahydrofuran or dimethoxyethane) have not been sufficiently transparent to give any signal by ir observation. Consequently, the complete lack of previous spectroscopic investigation in the infrared region can be attributed to the difficulties of the sampling techniques and the reactivity of the samples. It was not convenient to undertake an ir spectroscopic measurement without the technique whereby the complex is condensed to form a thin film on an infrared transparent substrate in a high vacuum. Even then, no chemical interaction between substrate and sample can be allowed.

The present work was designed to (a) develop a solid sample preparation technique via co-condensation to form a thin film on some suitable substrate in order that (b), (c) and (d) (see below) can be carried out; (b) investigate the optical properties using infrared and Raman methods to study the effect of electron transfer on molecular vibration for these particular donor-acceptor systems; (c) observe the electronic transitions

after formation of the complexes, i.e., absorption spectra in the visible region as well as laser excited emission spectra; (d) measure the resistivity of the complexes; (e) propose a description of the charge-transfer effect and the mechanisms of conduction and (f) suggest possible interpretations based on the established charge-transfer theory and from the spectroscopic results.

<div align="center">Past Experimental Studies and Interpretations</div>

Different sample preparation techniques can be expected to give different physical states of the complexes, which will lead to different optical and electrical properties and thus, different interpretations.

Sample Preparation Techniques

One can summarize the techniques used for preparation of samples according to the physical states of the complexes obtained from the various methods.

Complexes Formed in Inert Solvents. The addition of alkali metals to the polycyclic aromatic hydrocarbons was first studied intensively by Schlenk and Bergman (3). In 1936, Scott, Walker and Hansley (4) reported that reaction of sodium with naphthalene and other polycyclic aromatic hydrocarbons in dimethoxyethane leads to an intensely colored solution with relatively high electrical conductance. The existence of these electron transfer products were further evidenced by Weissman (5,6,7), Hoijtink (8,9,10) and their coworkers, who were able to prepare a large number of such solutions in tetrahydrofuran.

Isolated Solvent-Free Solid State Complexes. Holmes-Walker and

Ubbelohde reported preparation of solvent-free solid state complexes of lithium, sodium or potassium and anthracene as well as other solid intermolecular charge-transfer complexes (12,13,14,15,16). The preparation technique was difficult and lengthy. They were essentially prepared in inert solvents in an inert atmosphere, then isolated.
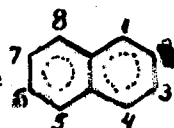
Complexes Formed Between Layers of Donors and Acceptors. In 1935, Suhrman (17) prepared the complex by evaporation of the hydrocarbons onto a previously deposited film of alkali metal. This technique was further applied by Inokuchi (18), Kearns (19,20) and Vaubel (21).

Characterization of Samples

Spectroscopic as well as electrical properties and the photo-electric effect were the earlier workers' primary interests.

Spectroscopic Characteristics. Electronic and electron spin resonance spectra of mono and di-negative ions of various arenes were reported by Hoijtink (8,9,10) and Weissman (5,6,7) in solutions. The absorption spectra in the visible and UV regions of solid layer complexes for sodium-anthracene and sodium-perylene were reported by Kearns (19, 20). There has been no successful infrared spectroscopic study either in solution or the solid state for these systems. The first investigation of infrared band shifts with odd electron density in the aromatic anion radicals was reported by Eargle and Cox (22) in solution. Only benzophenone, fluorenone and biphenyl radical anions were reported in some detail using dimethoxyethane as solvent. Further, no Raman spectroscopic investigations on metal-naphthalene system have ever been published.

Theoretical values from one-electron LCAOMO treatment of hydrocarbon negative ions were calculated by Hoijtink and co-workers (9) in order to determine the positions of the high free valency number for various arene anions, e.g., for naphthalene , the predicted positions of the highest charge density are equivalent at 1, 4, 5 and 8 for mono and di-negative ions.

Electrical Properties of Solid Complexes. These were investigated by Ubbelohde's group (12,13,14,15,16) in England. It was pointed out that the remarkable increase of conductivity which was found for aromatic hydrocarbons as electron acceptors with alkali metals as electron donors can be interpreted in terms of charge-transfer complexation which permits generation of carriers in the complexes more easily than for the parent aromatic hydrocarbon crystals. The proposed model for bonding between alkali metal atoms and the aromatic groups was quasi-metallic. The sodium rich complexes $Na_{(x)}A$ with $x > 2$ showed particularly marked enhancement of the pseudo-metallic properties. They were believed to consist of alkali metal atoms dispersed in solid solution in the crystal of the aromatic hydrocarbon with substantial, but not complete transfer of electron between alkali metal atoms and anthracene. A positive temperature coefficient of conductivity indicated that the electrons have to be activated to pass into a conducting energy band.

Photo-Electric Emission of Electrons From Alkali Metals Into Anthracene Crystals. This was first reported by Suhrman (17) in 1935 and 1937. Kearns (19,20) gave a comparison between absorption spectra and quantum yield of photoelectrons. Vaubel (21) reported a similar investi-

gation but with more extensive results using alkali and alkaline-earth

metals as electron donors in order to observe the second conduction band

in the anthracene crystals. The transfer of electrons from Cs, Na, Ca

and Mg to anthracene crystals can be released optically. This gives

rise to a spectral response which is nearly identical with the optical

absorption of the anthracene mono-negative ion was reported by Hoijtink et.

al (23) in the visible region. The spectral response curve for injection

of photo-excited metal electrons into the anthracene crystals is inter-

preted as a sum of two contributions. (i) Injection into the narrow

first conduction band and (ii) injection into a broad second band located

0.55 - 0.05 eV above the first one.

Other Physical Properties Such as Density, Magnetic Properties, Di-

electric Loss, Etc., Were Also Investigated. The results obtained were

used to confirm the dative nature of the salt-like crystalline solids of

the alkali metal-anthracene systems, but Ubbelohde et. al. concluded

that the electron transfer is not quite complete in the solid complexes.

Charge-Transfer Complexes

A simple charge-transfer reaction is defined as one for which no

bonds are broken or formed during an electron transfer step. Such reac-

tion might result in complex formation, or might be preceded or followed

by bond-breaking or bond-forming steps in a several step reaction mecha-

nism. For this study the interest is in the formation of complexes dur-

ing the charge-transfer process. The charge-transfer complexes are

characterized by either a partial or nearly complete transfer of electron

from donor to the acceptor, the amount of transfer being proportional to

the strength of the intermolecular interaction. This interaction accom-

panies the overlapping of the lowest unoccupied molecular orbital in the acceptor and the highest one in the donor. It has also been shown that the symmetry of the two molecular orbitals is an important factor in allowing charge-transfer interaction to take place (24). A quantum mechanical description of complex formation between various electron donors and acceptors was reported by Mulliken (25).

The interaction between alkali metals, odd-electron donors of low ionization potential, and π-electron acceptors of the relatively high electron affinity, results in essentially a complete electron transfer to form an odd-even ion-pair if the interaction is of 1:1 type. $Na^+ \cdot TCNE^-$ is a typical odd-even ion-pair. For other types of n:1 interaction where n > 1, the situation might be quite different. For example, the electron transfer might be less nearly complete; nonstoichiometric compounds may exist as solid solutions of alkali-metal-polycyclic aromatic hydrocarbon mixtures. In general, complex formation of nD:A (n donors of odd electron type to one acceptor of π structure type) where n may be 1,2,3, etc., is known to take place in the solid state (26,27,28,29) as well as in the gas phase (30).

Spectroscopic Characterization of Charge-Trans-
fer Complexes

One of the most direct and successful methods for investigating charge-transfer complexes has been the use of various spectroscopic techniques. Absorption of UV and visible light is probably the most widely used. A portion of the absorption spectra of molecular complexes in these regions, eg., HMB-TCNE (hexamethylbenzene-tetracyanoethylene) system, may be considered as resulting in electron transfer from the donor, HMB, to the acceptor, TCNE molecule (26). Very intense broad bands are

observed (31), which correspond to the so-called charge-transfer bands. They are characteristic of the molecular complexes with band positions dependent on both the acceptor (electron affinity) and the donor (ionization potential).

Infrared and Raman spectroscopic observations have also provided valuable information in the investigation of charge-transfer phenomena. In the present case the donor is the atomic metal which by itself is not associated with any molecular vibrations. Charge-transfer induced frequency shifts for the acceptor are determined by what type of orbital the transferred electrons enter, the most common case being transfer into an anti-bonding molecular orbital, which transfer tends to reduce the vibrational frequencies of the acceptor. The activation of certain vibrational modes in charge-transfer complexes, is another important phenomenon which can be observed experimentally and explained in principle. An example of this is the activation of the Cl_2 stretching mode upon complex formation with benzene (32,33,34). Resonance Raman scattering may also be observed if the excitation line falls in the electronic absorption band of the sample (see Chapter II).

Electronic Transitions

Electronic transitions for charge-transfer complexes can be summarized into two categories according to the nature of the observable transitions.

(a) Thermal activation of electrons from the highest filled band to the lowest unoccupied conduction band of solid charge-transfer complexes causes a typical intrinsic semiconductive behavior. The conduction mechanism can be explained in terms of a band structure in the case

that a linear relationship exists between log conductivity and the reciprocal of temperature. Therefore, the generation of charge carriers is a necessary process for the conduction to occur. Most organic semiconductors are found to belong to this case. On the other hand, highly conductive anion-radical-types of organic semiconductors have been found for which little or no thermal activation is required for conduction to occur, although a linear relationship still holds (35). It has been proposed to interpret this observation in terms of either a hopping model or tunneling (36).

(b) Internal optical transfer from donor to acceptor of an electron in a charge-transfer complex during excitation from the ground state to the excited singlet state or vice-versa with a resulting absorption or emission. The spectra observed in the visible region of colored complexes can usually be attributed to this optical activation.

CHAPTER II

THEORETICAL CHARACTERIZATION OF MOLECULAR

CHARGE-TRANSFER COMPLEXES

The theory of donor-acceptor complexes and their spectra, as orig-
inated by Mulliken (25), is a vapor state theory with omission of London-
dispersion terms. The application of this theory to weak complexes in
solutions, after small corrections for solvation energies has been proven
to be essentially valid in inert solvents. Experimental results for
many solid complexes can be understood in terms of the simplified theory
as well.

Complexes formed between donor-acceptor pairs resulting from charge-
transfer without either the dissociation or formation of bonds, which
are classified as dative or weak, can be distinguished by spectroscopic
studies, particularly, if the sampling technique is favorable for infra-
red investigation. Complexes are classified as dative if the infrared
spectrum is considerably different from that of either constituent molecule
(29) and, in particular, if it resembles that of the anion (cation), as
in the case of the alkali salts of semiquinones (29). On the other hand,
if the infrared spectra of the complexes show a close resemblance to the
uncomplexed entities, the complexes are considered to be non-ionic or
weak; for instance, the benzene-iodine complex (37).

The structural characterization of complexes via a spectroscopic
approach as well as conductivity studies is emphasized in this chapter.

The former includes visible, infrared, Raman and resonance Raman and emission spectra; the latter concentrat on the enhanced semiconduction.

Electronic Transitions

Electronic Absorption Spectra

Electronic absorption spectra for molecular complexes can be summarized under three types, i.e., charge-transfer spectra observed mostly from non-ionic complexes; spectra inherent to the anions and/or the cations from dative complexes dissociated in polar solvents; the associated salt spectra at low temperature either in solutions or in crystalline solids.

The major part of donor-acceptor interaction theory has been presented in terms of a single pair of electrons or just one electron in the case of odd-even complexes. A characteristic indication of the formation of charge-transfer complexes is the appearance of new broad optical absorption bands which can not be attributed to donors and acceptors separately. The excitation of such complexes may be associated with the partial or complete transfer of an electron from donor molecule to the acceptor. A number of equations have been proposed for relating the frequency of the maximum in the absorption of the charge-transfer complexes to the characteristics of the donor and/or acceptor.

It is of interest to consider the complexes that are formed between alkali metal (M) and polycyclic aromatic hydrocarbons (Ar). The essential features of this type of complex can be described by using one-electron approximation. The wavefunction of this complex in the ground state, is given in general by

$$\Psi_N = a\psi_0 \ (Ar^-, \ M^+) + b\psi_1 \ (Ar, \ M)$$

$$\text{or} \quad \Psi_N = \psi_0 \ (Ar^-, \ M^+) + \lambda\psi_1 \ (Ar, \ M), \ \lambda = b/a$$

where $\psi_0 \ (Ar^-, \ M^+)$ represents the dative structure in which an unpaired electron occupies the lowest anti-bonding molecular orbital of the aromatic hydrocarbon molecule, and the alkali metal is positively charged; $\psi_1 \ (Ar, \ M)$ represents the charge-transfer structure, (with no bond) and λ the mixing parameter. According to the second-order perturbation theory, λ is much less than 1 and is given by (38,39)

$$\lambda = -W_{10}/(I_D - E_A + e^2/\bar{r})$$

where I_D and E_A denote the ionization potential of the donor and the electron affinity of the acceptor molecule respectively, and $e^2/\bar{r}$ the average electrostatic energy between the radical anion and the cation, and W_{10} is defined as $\langle\psi_1|H|\psi_0\rangle$. One can classify this complex as an anti-bonding donor and vacant acceptor type. The simplified resonance structure for the charge-transfer excited state is given by

$$\Psi_V = a^*\psi_0 \ (Ar^-, \ M^+) + b^*\psi_1(Ar, \ M)$$

$$\text{or} \quad \Psi_V = \psi_0 \ (Ar^-, \ M^+) + \lambda^*\psi_1 \ (Ar, \ M)$$

where λ^* is $\simeq 1.0$.

Applying basic quantum mechanical arguments the charge-transfer excitation energy $(h\nu_{CT})$ is given as

$$h\nu_{CT} = W_V - W_N = 2\sqrt{(\Delta/2)^2 + \beta_0\beta_1}\Big/(1-S_{o1}^2)$$

where W_V is the energy of the excited state, and W_N is the energy of the ground state,

$$\Delta \equiv W_1 - W_o, \text{ and } W_1 = \langle \psi_1^* |H| \psi_1 \rangle, \quad W_o = \langle \psi_o^* |H| \psi_o \rangle,$$

$$W_{o1} = \langle \psi_o^* |H| \psi_1 \rangle, \quad \beta_o = W_{o1} - W_o S_{o1}$$

$$\beta_1 = W_{o1} - W_1 S_{o1}, \quad S_{o1} = \langle \psi_o^* \psi_1 \rangle$$

Using second order perturbation theory, $h\nu_{CT}$ is then approximated as

$$h\nu_{CT} \approx \Delta + \frac{\beta_o^2 + \beta_1^2}{\Delta} = \Delta + X_o + X_1$$

where $\beta_o^2/\Delta, (X_o)$ and $\beta_1^2/\Delta, (X_1)$ are the resonance energy of the ground state and the excited state at equilibrium separation, respectively. One may now estimate Δ with the help of experimentally available data, since in Figure 1
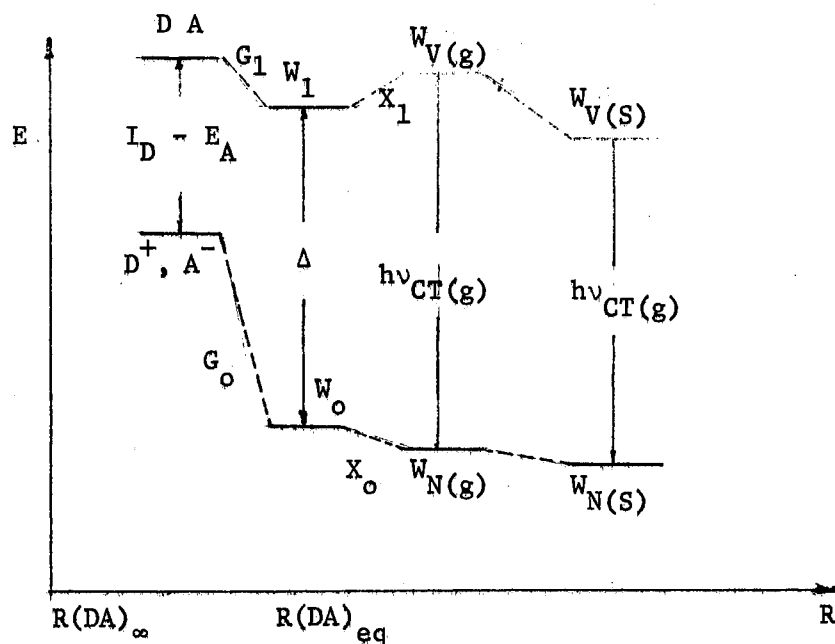
Figure 1. Energy Level Diagram of Charge-Transfer Process

the G's are the coulomb energy, X's are the resonance energy; g, repre-
sents gas phase; s, represents the solid state.

From experiment, the hydrocarbon negative ions are formed by adding
one or two electrons to the π-electronic systems of the corresponding
polyacenes from chemical or electrochemical reduction. Spectroscopic
information about the existence of these anions either as free negative
ions or as anions which are associated with alkali metal cations has
been obtained by various workers (5-21,23,40). It is therefore, neces-
sary to consider the nature of the electronic transitions in the visible
and ultra-violet regions. In most cases, the observed electronic transi-
tions have been assigned to internal transitions, i.e., the absorption
spectra were attributed to electronic states of the anions either sol-
vated or ion-paired with a cation. These anion spectra furnished a test
of the chemical bonding theories. Thus Hoijtink et. al. have calculated
the bond order change of the various aromatic hydrocarbon anions (9) as
well as the theoretical transition energies (23) for comparison with the
observed spectra in liquid and rigid solutions.

One could imagine that there exist spectral shifts from neutral
polycyclic aromatic hydrocarbons to the mono- or di-negative ions of the
corresponding polyacenes as a result of one or two electron-transfer.
Theoretical investigations have found that a red shift from U.V. to vis-
ible is expected for all the linearly condensed ring systems. Other in-
teresting questions are concerned with where the odd electron is located and
where the cation is to be found in the case of association. Hoijtink et al.
have argued that the transferred odd electron is delocalized with cer-
tain positions having higher charge densities, and that the cation in
the ion-pair is not centered on the molecular plane, but offset along

the longer axis (in order to interpret the spectral intensity change (23)).

Luminescent Spectra

After absorption of light, the excited complex may be expected to dissipate its excess configurational energy and to move toward the equilibrium configuration of all the vibrational coordinates. For example, luminescent spectra have been observed using thin films of co-deposited potassium-anthracene complexes (11). This corresponds to the inverse transition which involves charge-transfer from the no-bond excited state to the dative ground state, and, normally, a spectrum, that is a mirror reflection of the charge-transfer absorption (41).

Consider the process of excitation for which, the electron transfer

$$A^+ \cdots\cdots D^- \xrightarrow{-h\nu_{CT}} A,D$$
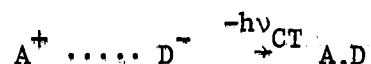
causes a considerable change of the interaction energy of the components. In the ground state a strong attractive force caused by electrostatic interaction is involved, while in the excited state, the attractive energy of the uncharged pair is quite weak.

Figure 2 represents the potential curves to illustrate the Frank-Condon (FC) principle. All q's are adjusted through internal conversion so as to minimize the energy $E_N(R, q_g)$ and $E_V(R, q_v)$, and causing $h\nu_{CT}^{em}$ to be $< h\nu_{CT}^a$.
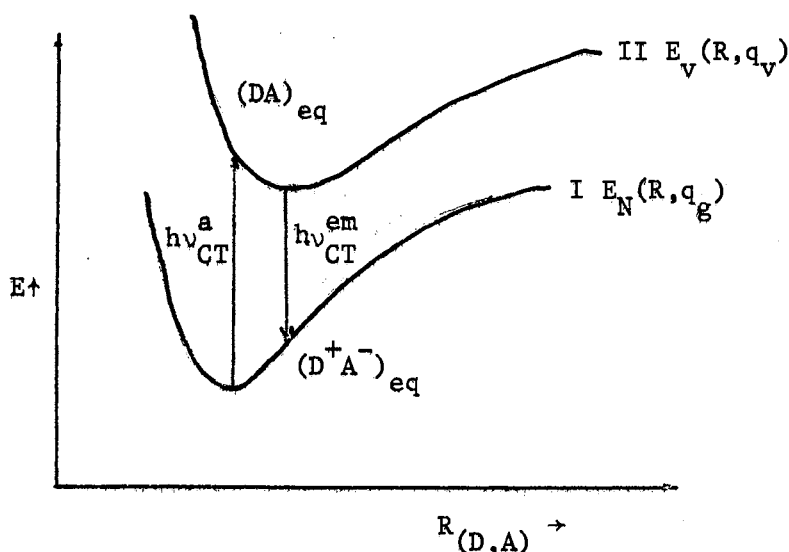
Figure 2. Schematic Potential Curves
Illustrating Frank-Condon
Principle

There is some difference between the equilibrium distance R_{eq} of

the ground state and R_v of the excited state, here, in Figure 2.

R is the distance between the complex components. Curve I represents

the potential energy of $(D^+ A^-)$ in its ground state, $E_N(R, q_g)$, where q_g

are the configurational coordinates. According to the FC principle, the

maximum of the observed charge-transfer absorption band corresponds to

approximately vertical transition. But in the excited state, $E_v(R, q_v)$,

the complex minimizes the excess vibrational energy of the FC configura-

tion. Fluorescence is then expected to occur from the equilibrium con-

figuration of the excited electronic state to the ground electronic

state, and $h\nu_{CT}^{em}$ will be lower than $h\nu_{CT}^{a}$. Fluorescence spectra of the

internally excited anions will follow the same principle and the details

will be discussed in Chapter IV. A possible fluorescent mechanism for

metal-doped aromatic hydrocarbons, such as anthracene and naphthalene,

is as follows: The aromatic hydrocarbon molecule, Ar, is reduced to the

anion radical by accepting an electron

$$Ar + e \rightarrow Ar^-$$

If Ar^- is excited by absorbing some radiation (hν)

$$Ar^- + h\nu \rightarrow (Ar^-)^*$$

or
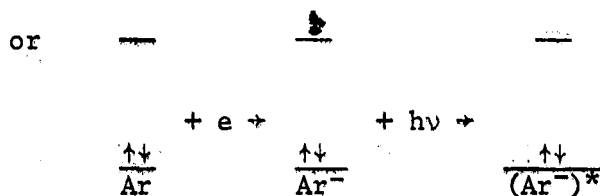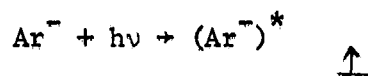
and there are excess neutral aromatic hydrocarbon molecules, then energy transfer is possible

$$Ar + (Ar^-)^* \rightarrow (Ar^-) + {}^1(Ar)^* \text{ and/or } {}^3(Ar)^*$$
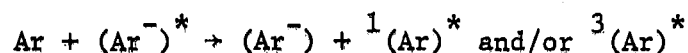
and one might have assisted fluorescence and/or phosphorescence. Further, the presence of the pure anionic form of the arenes, would eliminate this possibility.

Vibrational Spectroscopic Aspects of the Charge-Transfer Complexes--Infrared and Raman Spectroscopic Observation

Infrared Spectra of Charge-Transfer Complexes

Infrared spectra may undergo the following possible changes when a charge-transfer complex is formed with transfer of an electron from the donor to an anti-bonding orbital of the acceptor:

(a) frequency shifts;

(b) intensity change and broadening of the bands;

(c) activation of certain inactive modes in the infrared spectra;

(d) new low frequency bands of DA pairs or crystals;

(e) elimination of the correlation field coupling in the solid state through separation of neighboring like-molecules;

(f) vibronic wash-out.

In the case of $(Ar^- M^+)$ system, it has been found experimentally that the system in THF solution exists entirely as ion pairs (23). The vibrational spectra of these complexes which will be expected to be considerably different from that of the neutral parent molecules are particularly useful in further understanding the nature of the complexes and particularly the bonding changes in the Ar^-. Electron spin resonance studies and semiconductive data suggest that the transferred electrons are not entirely on the arene molecules (39).

A theoretical explanation of the behavior listed under (a), (b), (c) and (d), particularly for weak complexes, has been reviewed by Mulliken (42), and application of the theory has proven to be satisfactory for weak complexes. In general, the change of bond order or, in other words, the change in the magnitude of the force constants is the basis for the interpretation of the observed spectra. Bond order may be regarded as a relative measure of the shared electrons effectiveness in holding two atoms together. It must be related to force constant size. Theoretical prediction of the bond orders for neutral arenes and anions of arenes have been made with the aid of Hückel's treatment by Hoijtink (8,9). Scherer (43) has been able to show that the application of a modified Urey-Bradley force field for condensed aromatic rings leads to some remarkable conclusions regarding the vibrational spectra.
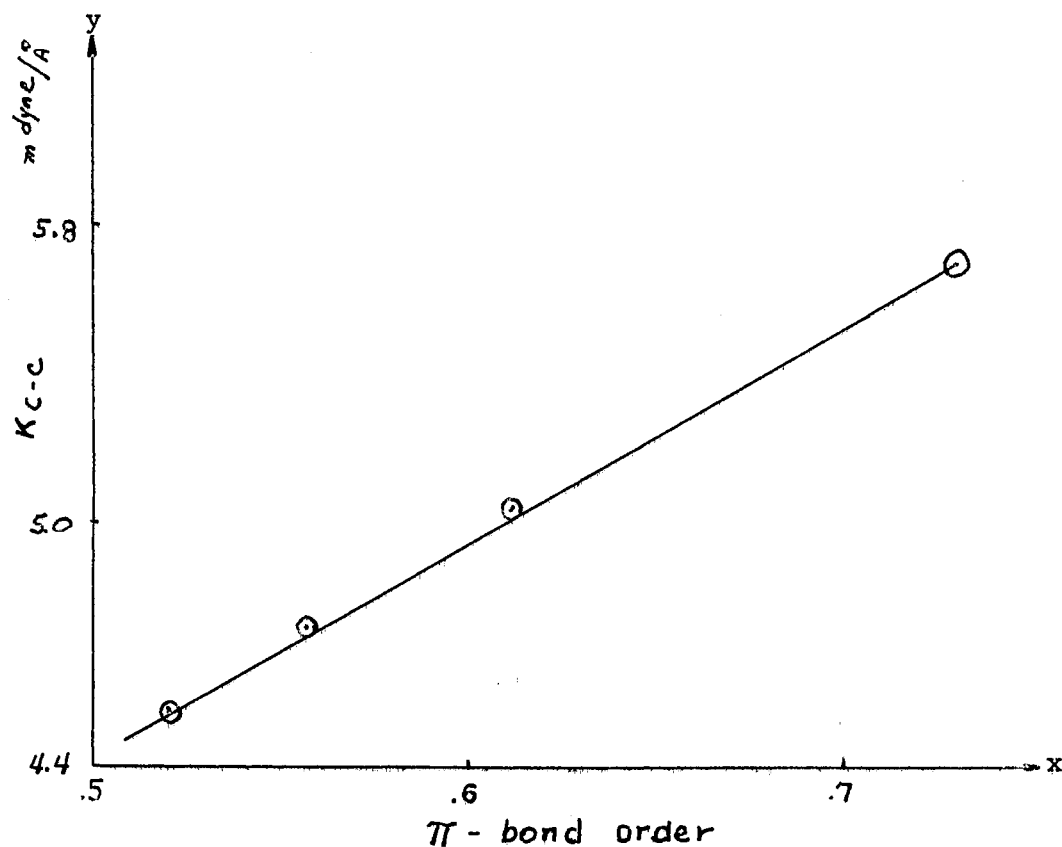
Figure 3. Plot of Force Constants Versus π-Bond Order

Scherer (43) specified the potential function arising from the interaction of the π-electrons with bond stretching coordinate R, so that, in matrix notation

$$2V_R = R' (F_{UBFF} + F^{\pi R}) R$$

where $F^{\pi R} = \rho f^{\pi R}$, and ρ is a scalar variable. It is plausible to propose that the additional potential function arising from the interaction of the transferred electron with the bond stretching coordinate R of the anion is

$$\mathbf{F}^{(\pi)'R} = \rho \cdot \mathbf{f}^{\pi'R}$$

therefore,

$$2V_{\overset{\cdot}{R}} = 2V_R + \mathbf{R}'(\mathbf{F}^{(\pi)'R})\,\mathbf{R}$$

where $\cdot$ signifies the odd electron. Assuming that the Kekülé resonance structures are of equal importance, and also that the anion has the same symmetry as the neutral molecule with the negligible variation of the bond length and bond angle, it is then possible to calculate the force constants using the observed vibrational frequencies from both Raman and infrared spectra.

(a) (b) (c)
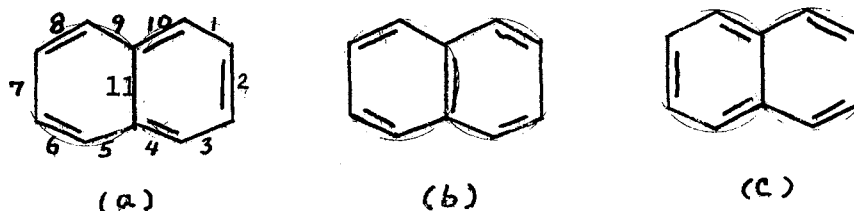
If one considers only the C-C stretching force constants of bonds 1, 2, 10 and 11, a plot of the calculated values of π-bond orders versus C-C stretching force constants, K_{C-C}, can be obtained. An approximate linear relationship is thus apparent from the graph in Figure 3. This linear relation has been assumed by Gordy (44), i.e.,

$k = f(N, \chi_A, \chi_B, d)$ where k is the stretching force constant, N is the π-bond order, χ_A, χ_B are electronegativity of element A and element B, and d is the bond length. The empirical relation is

$$k = aN \left(\frac{\chi_A \cdot \chi_B}{d^2}\right)^{3/4} + b \, .$$

Both calculations have been based on Hückel molecular orbital theory al-

though by different authors. One can further assume that, if this relation also holds for the mono-negative ion of naphthalene, then, qualitative zero order force constants of the anion can be obtained using the graph and Hoijtink's anion bond orders as a guide. Improved force constants can then be calculated by fitting the observed frequency shifts of the vibrational modes.

The activation of infrared inactive modes as well as intensity changes when donor and acceptor molecules come together can be explained in terms of the "electron vibration" (model)(26,27,28,32,33,34) which considers the highly polarizable electron cloud on the radical anion. The electron cloud is distorted by the presence of the point cation and the variation of the anion charge cloud polarizability with totally symmetric vibrations produces an effect such that the magnitude of the directed dipole between anion and cation oscillates. Thus, the mode is activated. By contrast the effect of vibronic wash-out is the extensive cancellation of the normal vibrational transition moments as a result of the response of the electron to those moments. For example, the radical electron of a TCNE (tetracyanoethylene) anion, when viewed as a particle in a box, appears capable of wiping out the normal infrared activity of the anion (27,28).

It has been pointed out by Jones (45,46) that the intensity contribution from the delocalization of the π-electron in the vibrational spectrum of the even-alternant hydrocarbons is small. In other words, the delocalizing π-electrons in the even-alternant hydrocarbons do not significantly affect the dipole derivatives for the C-C skeletal motions. Experimental infrared spectral results of benzene and naphthalene support the theoretical prediction fairly satisfactorily.

In the case of an anion radical or a charge-transfer complex, the intensity change as well as the frequency shifts of certain vibrational modes depend on a number of factors, i.e., the redistribution of the electron cloud due to the presence of the transferred electron on the anion; the interactions between anion and cation and the change of symmetry of the molecule. Therefore, the transition moment of certain vibrational modes in the neutral molecule might be greatly enhanced, canceled or changed very little after formation of the complex as a result of the response of the transferred electron and the vibration. Ferguson and Matsen (75,76) and Friedrich and Person (77) have shown that the vibration of atoms carrying fixed charges cannot by itself account for the infrared intensities observed in charge-transfer complexes. The enhanced intensity is attributed to a "delocalization moment," arising from vibronic interactions. Such delocalization moments may have more pronounced effects in the charge-transfer complexes than in the neutral even-alternant hydrocarbons.

New low frequency motions in the complexes are expected in which D vibrates against A. In the M, Ar systems for 1;1 and 2;1 complexes, these new vibrations are expected to fall in the far infrared region. Very sparse information in this area has been obtained due to lack of proper instrumentation (73,74).

Raman Spectroscopic Study of Charge-Transfer Complexes

A complete understanding of vibrational aspects of charge-transfer complexes must include the Raman spectrum which provides useful data not only complimentary to what is obtained from infrared spectroscopy, but also gives new information concerning vibronic interactions and the res-

onance Raman effect.

Placzek (47) points out that, owing to the relatively large mass and slow response of the atomic nuclei, Raman scattering is normally due practically entirely to the electrons. It is, therefore, expected that the change of the electron density upon transferring an electron from the donor to the acceptor will produce Raman scattering which is noticeably different from that of the neutral substance.

Classically, the electrical moment is induced in the scattering molecule by the electric field E of the incident light. If α is the molecular polarizability, one may write

$$\vec{P} = \alpha\vec{E} \tag{2-1}$$

here $\vec{P}$ is a vector of the induced moment, and α is time dependent, because of molecular vibration.

In a quantum mechanical approach, it is necessary to consider the matrix element $\vec{P}_{nm}$ for the transition n←m in question instead of the classical induced moment.

$$\vec{P}_{nm} = (\int \psi_m^* \alpha\psi_n \, dt)\cdot\vec{E} = \alpha_{nm}\cdot\vec{E} . \tag{2-2}$$

If one considers only vibrational wavefunctions and α is regarded as a function of only nuclear coordinates, then $\vec{P}_{nm}$ is a vibrational transition moment. For a particular vibrational mode, Placzek expanded α as a Taylor series in the displacement coordinate. Dropping off higher order terms and applying the vibrational wavefunction for simple harmonic motion gives

$$\alpha_{n,n+1} = \int \psi_{n+1}^* \alpha_0 \psi_n \, d\theta + \left(\frac{\partial\alpha}{\partial\theta}\right)_0 \int \psi_{n+1}^* \theta \psi_n \, d\theta \tag{2-3}$$

upon integration,

$$\alpha_{n,n+1} = (\frac{\partial \alpha}{\partial \theta})_0 \sqrt{\frac{(n+1) \ h}{8\pi^2 \mu \nu}} \qquad (2\text{-}4)$$

where μ is the reduced mass and, ν the fundamental frequency. The intensity of scattering of the mode at right angles relative to the incident light is given by

$$I = N_n \frac{64\pi^2}{3 \ c^2} (\nu_0 - \Delta \nu)^4 (P)^2_{nm} \qquad (2\text{-}5)$$

Thus, inelastic collision between molecules and photons may cause a molecule to undergo a quantum transition to a higher energy level, with the result that the photon loses energy and is scattered with lower frequency. If the molecule is already in an energy level above its lowest, the collision may cause it to undergo a transition to a lower energy, in this case the photon is scattered with increased frequency $(\nu_0 \pm \nu_{mol})$.

It has been known for years that Raman spectral features observed when the frequency of the exciting light approaches or enters the region of the electronic transition of the molecules, may be of unusually high intensity as the result of the resonance Raman effect. The intensity theory of equation (2-5) is no longer valid. A semiclassical theory developed by Shorygin (48) is briefly introduced. When the incident light frequency ν is near to an electronic absorption band, the polarizability derivative is given by

$$|\alpha'| = \frac{z^2 \ f_e \ \nu_e \ \nu'_e}{2\pi^2 c^2 m \ [(\nu_e^2 - \nu^2) - \nu^2 \gamma_e^2]}$$

and scattered intensity will depend on the square of $|\alpha'|$. Here z is the charge of the electron; m, the mass of electron, f_e, the electronic transition oscillator strength calculated from the absorption band area, ν_e, the frequency of the electronic absorption maximum in cm^{-1}, γ_e, the attenuation coefficient; c, the velocity of light; ν, the exciting frequency. The second derivative of α corresponds to the intensity of the overtone band.

In the rigorous resonance Raman effect the intensity of Raman lines (including overtones and combination tones) depends on the position of the exciting line relative to the single vibrational maxima of the electronic absorption band. An extended overtone structure in the resonance Raman spectrum may be observed only when the exciting frequency falls into the interior of the distinctly observable vibrational structure of the absorption band (48).

Resistivity of Charge-Transfer Complexes

The decrease in resistivity of charge-transfer complexes in M, Ar systems as compared with neutral arenes can be related to the change of the activation energy ε_{act}

$$\rho = \rho_0 \, e^{\varepsilon_{act}/2kT}$$

where ρ_0 is a constant and ε_{act} is the activation energy for the conduction to occur, if the material has a semiconductive property.

The Band Model

In a weak complex, the intermolecular charge-transfer interaction is relatively weak in the ground state and the relation between log ρ_0 and

$\frac{1}{T}$ holds very well. The conduction mechanism for most of these complexes is explained using a band model. If the charge-transfer band maximum and the energy of activation are available, the relation between $h\nu_{cT}$ and ε_{act} can be expressed as

$$\varepsilon_{act} = h\nu_{cT} \text{ (solid)} - \Delta$$

where Δ is nearly constant in a group of molecular complexes with fixed acceptor if the donors are of the same type (49).

The conduction band may be assumed as one formed from the overlapping between the highest filled MO's of the donor molecules and the lowest empty MO's of the acceptor. Therefore, it results from the charge-transfer.

The Hopping Model or Tunnel Model

The related mechanisms for semiconduction in molecular crystals were proposed by Eley, Parfitt, Perry and Taysum (50) in 1953 and by Eley and others in 1955 (52). The proposed model for tunneling is sketched in Figure 4.

An electron can only move into an energy level which already contains less than two electrons. In (a) an electron denoted by X received energy $\Delta\varepsilon$ to excite it to an upper level from which it can pass (broken arrow) to the next molecule. The empty space set free in the lower level is taken up by an electron from the next molecule. In (b), the interaction between the excited states in the neighboring molecules broadens the upper level into a band, hence lowering the energy gap $\Delta\varepsilon$. In (c), a solid free radical, the electron can pass directly (broken line) into the corresponding level of the next molecule.
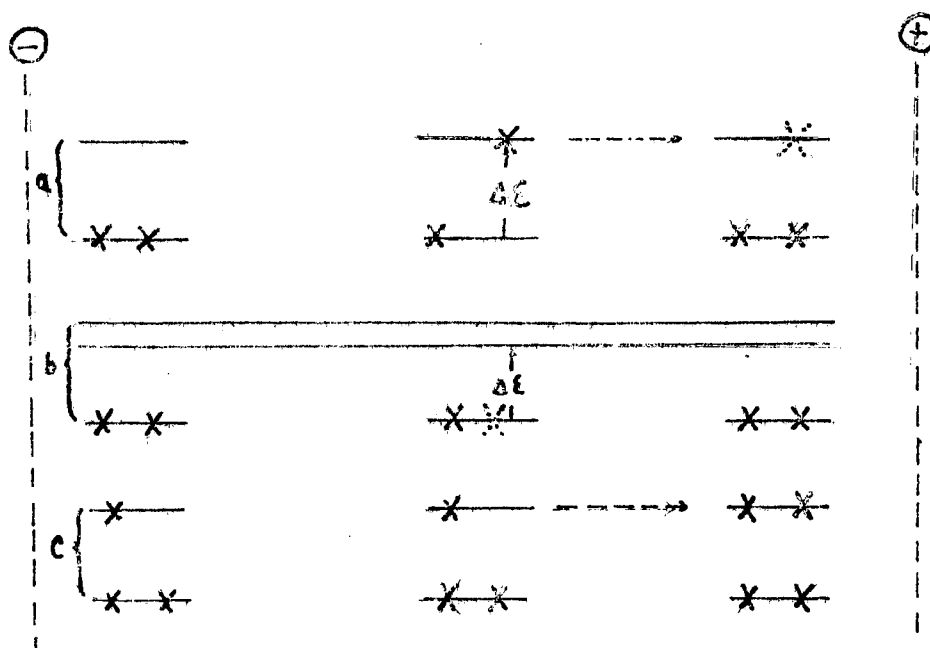
Figure 4. Schematic Representation of Tunneling Model
for Electrical Conduction in Molecular
Solids

In solid salt-like-charge-transfer complexes containing radical

anions associated with a cation, there is already an unpaired electron

on each of the adjacent molecular sites which can tunnel without prior

excitation. Eley and Parfitt (52) deduced that, if the simple tunnel

model were essentially correct, crystals of organic free radicals should

have a zero energy gap. The relatively low value of the energy gap in

$\sigma = \sigma_0 \exp(-\varepsilon_{act}/2kT)$ which they obtained for crystals of $\alpha,\alpha,$-diphenyl-

para-picryl hydrazyl (D.P.P.H.) a free radical
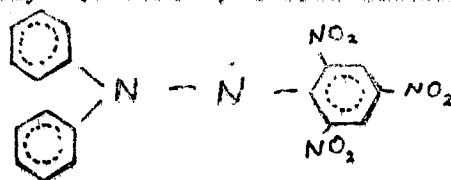
was evidence in support of the tunnel theory. Most free-radical types

of molecular crystals have a relatively low energy of activation. The

fact that it was not actually zero was attributed to the intercrystallite

defects (52).

It is assumed that for conduction to take place in a molecular crystal, it is necessary to ionize a molecule removing the electron until its coulombic energy is negligibly small (compared to kT, the thermal energy).

Eley, Inokuchi and Willis (53) applied the tunnel model to the complexes made by combining D with A (N,N-dimethylaniline, α-chloroanil). The solids contain D and A molecules arranged alternatively within stacks (54). The increase in conductivity is usually thought to be caused by changes in both quantities, σ_0 and ε_{act}, appearing in

$$\sigma = \sigma_0(T) \exp(-\varepsilon_{act}/kT)$$

since a charge carrier "sees" an ion-dipole as well as the ion-induced dipole forces.

CHAPTER III

EXPERIMENTAL APPROACH TO THE PREPARATION

AND CHARACTERIZATION OF POTASSIUM-

NAPHTHALENE COMPLEXES

The experimental techniques employed in this investigation can be divided into two main parts, i.e., sample preparation via co-condensation techniques and sample characterization via spectroscopic and electrical methods.

Sample Preparation and Apparatus

Co-condensation of two molecular (or one atomic and the other molecular) beams onto a suitable substrate in a high vacuum has been extensively applied throughout this experimental work. Co-condensation requires a high vacuum system and a cell in which two crossed molecular beams can be generated by using internal heaters. In addition, the cell has a construction such that multifold characterization of the sample can be carried out in one run. Samples of potassium-naphthalene complexes are extremely reactive toward traces of moisture and oxygen, so all characterization was done under high vacuum in situ so as to eliminate contamination.

The apparatus constructed for this study is essentially an extension of the work by previous investigators (27,28). Since the original design was for infrared spectroscopic investigations, a simple

cold finger was satisfactory. The present experimental work, which includes the observation of electrical as well as various optical properties of each sample, required special attachments to the cold finger. They are:

(a) A CsBr prism for visible (transmission) and infrared (transmission and atr) spectroscopic studies (Figure 5 a).

(b) An Al wedge for laser-Raman scattering and laser fluorescence excitation by the single reflection technique (Figure 5 b).

(c) A quartz plate with four strips of deposited gold for electrical measurements using a four-point-probe (Figure 5 c).

One can thus obtain spectra which cover both the visible and the infrared regions. Further one may expect to observe fluorescence and resonant Raman scattering as well as the ordinary Raman spectra if a proper choice of sample thickness and excitation frequencies are made.

The use of the cell requires a combination of high vacuum and good practice. Cell design was conceived with the intention that one might be able to treat a large number of chemical systems, either organic, inorganic or both, regardless of the physical state prior to deposition, (i.e., gas, liquid or solid) and obtain quantitative as well as qualitative information without further extensive reconstruction of the cell. The radiation from the heaters as well as the unwanted sample beams before and after deposition, must be limited and terminated effectively. Therefore, the two heaters were shielded by aluminum foil and the substrate of the cryotip was partially protected by a cylindrical copper shield (Figure 5 d). Furthermore, the crossed molecular beams could be stopped by another shield which was attached on a separate cold finger between the beam sources and the substrate (Figure 5 e). The angle of the

(b)
Al wedge

front view

(b) back view

Cu holder

atr prism

(a) CsBr prism for infrared
and visible absorption
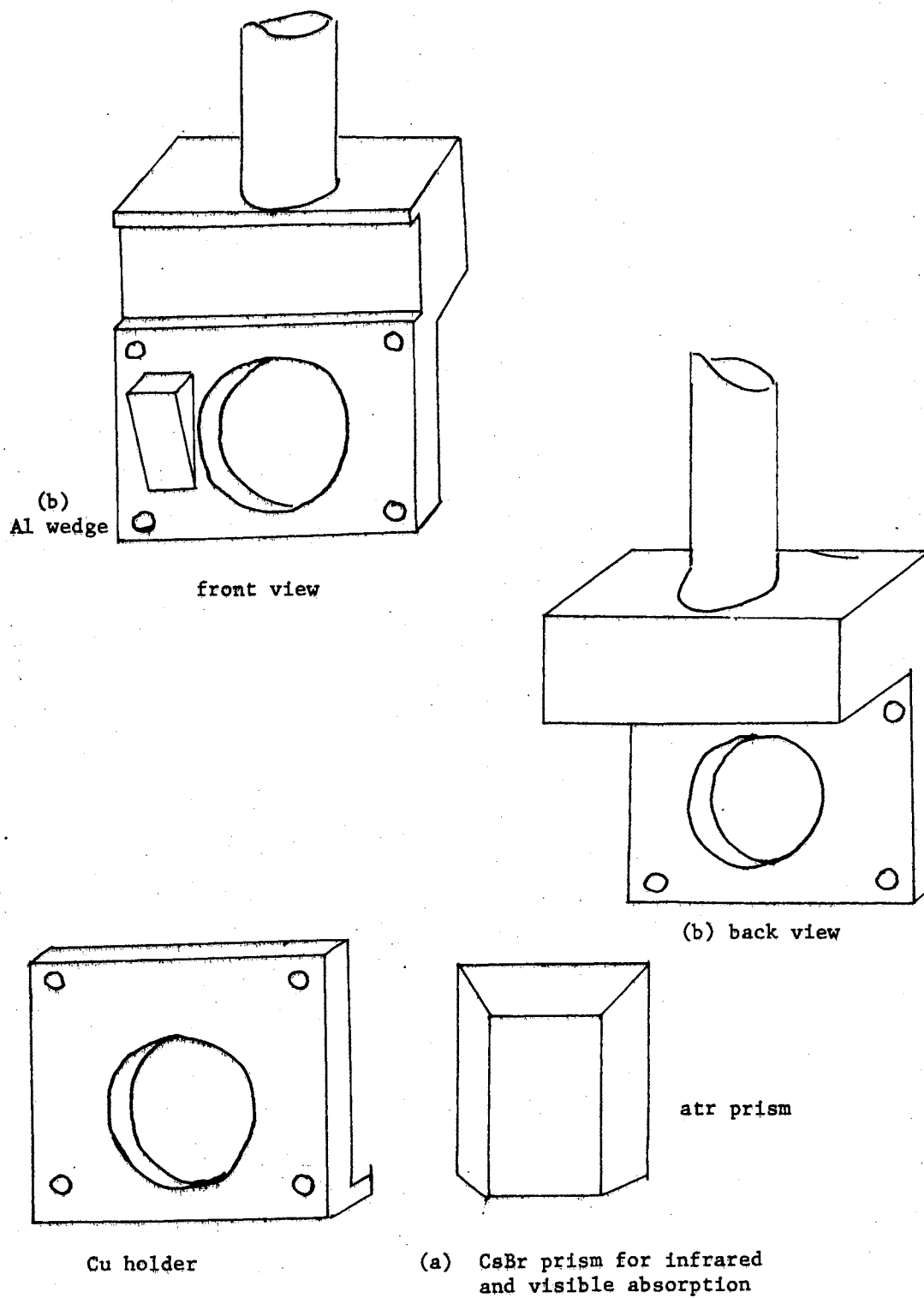
Figure 5. Special Attachments for the Cold Finger
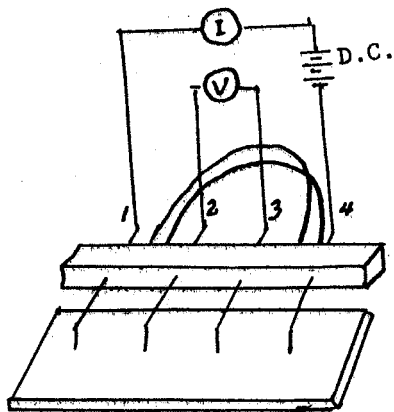
(c) the four-point-probe and the quartz substrate

(e) curved shield

light path of atr

conductivity

light path for infrared and visible transmission

light path of laser Raman spectrum
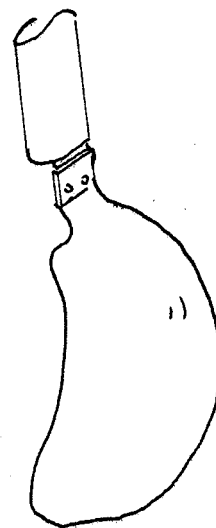
d. cylindrical shield
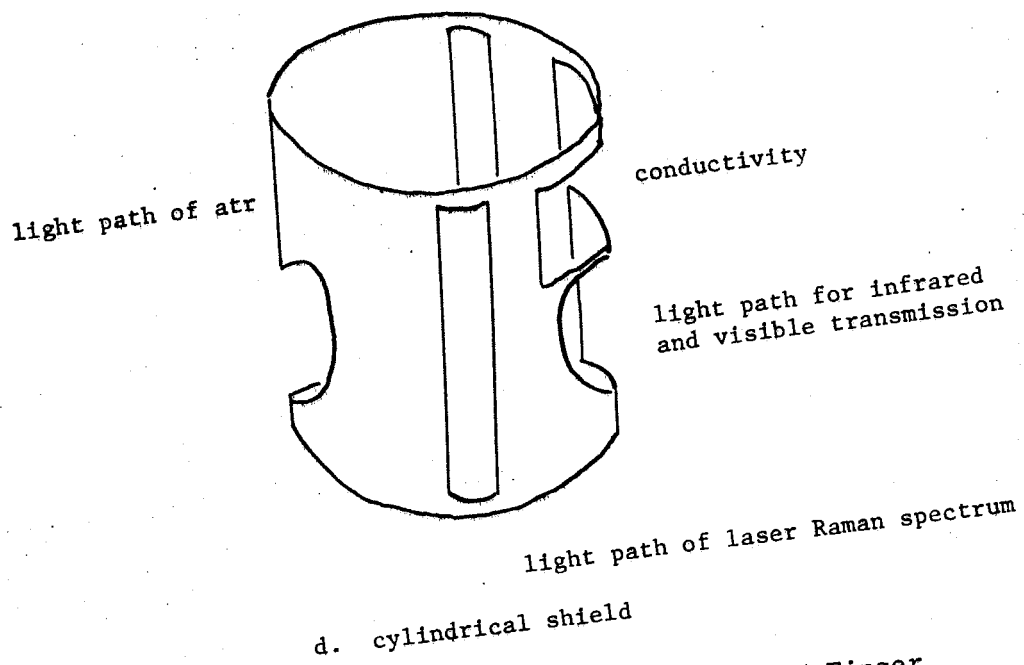
Figure 5. Special Attachments for the Cold Finger

crossed beams as well as the distance between the Knudsen cells (Figure 7) and the substrate could be adjusted providing greater versatility in sample preparation.

Several precautions require attention as one starts to prepare the experiment. First, the CsBr prism as well as the outer windows should be polished flat and be clearly transparent; second, the cleaned Raman wedge must be kept free from contamination by grease that causes a severe fluorescent background; third, the many electrical contacts should be tight. In the construction of the four-point-probe, it is especially necessary that all four probes are pressed firmly against the four gold strips with probe distances approximately equal. Since all measurements are carried out in high vacuum by passing either electrical current through the sample on the quartz plate or impinging photons on the samples to observe various spectra, cleaning of the cold finger as well as the rest of the cell is absolutely necessary before the system is completely assembled.

The second cold finger was used as a cold trap and sample barrier. A curved copper shield, which was attached on the second cold finger in such a way that it could be rotated to either side of the molecular beams during deposition, was placed in front of the two heaters in order that unwanted beams could be prevented from depositing on the sample substrate. This shield did not guarantee that sample would not pass around the shield, if pressure was greater than 10^{-4} torr. Furthermore, the distance between the sources of the sample beams and the cold finger, as well as the angle between the crossed molecular beams, was critical in obtaining uniform depositions. For detailed considerations

one is referred to Anderson (1).

The control of vapor pressure by adjusting the heater temperatures or the pin hole sizes of the Knudsen cells could only be very roughly applied as an indication of an organic-rich or a metal-rich sample character. However, the failure to confirm the true beam density did not prevent the preparation of fairly pure solid complexes, an identification justified by the presence of a consistency in the characteristic vibrational spectra which could be varied during the repeated runs under similarly controlled conditions by the variation of the two experimental parameters.

Figure 5 a and b demonstrates how the center CsBr prism was mounted on the cold finger. The four-point-probe was also clamped to the brass support. The quartz conductivity plate, with four strips of deposited solvent-free liquid-bright-gold, was slipped into the trough on the cryotip, where four electrodes pressed against the four strips. An iron-constantan thermocouple wire was inserted for measuring the temperatures of the deposits. The cylindrical shield was mounted in such a way as to allow the Al wedge to be installed and was aligned to a position such that both transmission and atr (attenuated total reflection) spectra could be investigated.

The clean glass plate was clamped to the bottom of the main cell body (Figure 6 a) for laser beam entrance. The Knudsen cells, one containing the organic, the other containing alkali metal in n-heptane were put into the ohmic ovens. With an iron constantan thermocouple wire in each of the ovens, the ovens were connected to the copper outer cell plate II (Figure 8). All electrical connections were completed with no distortion on the four-point-probe before the whole apparatus was closed
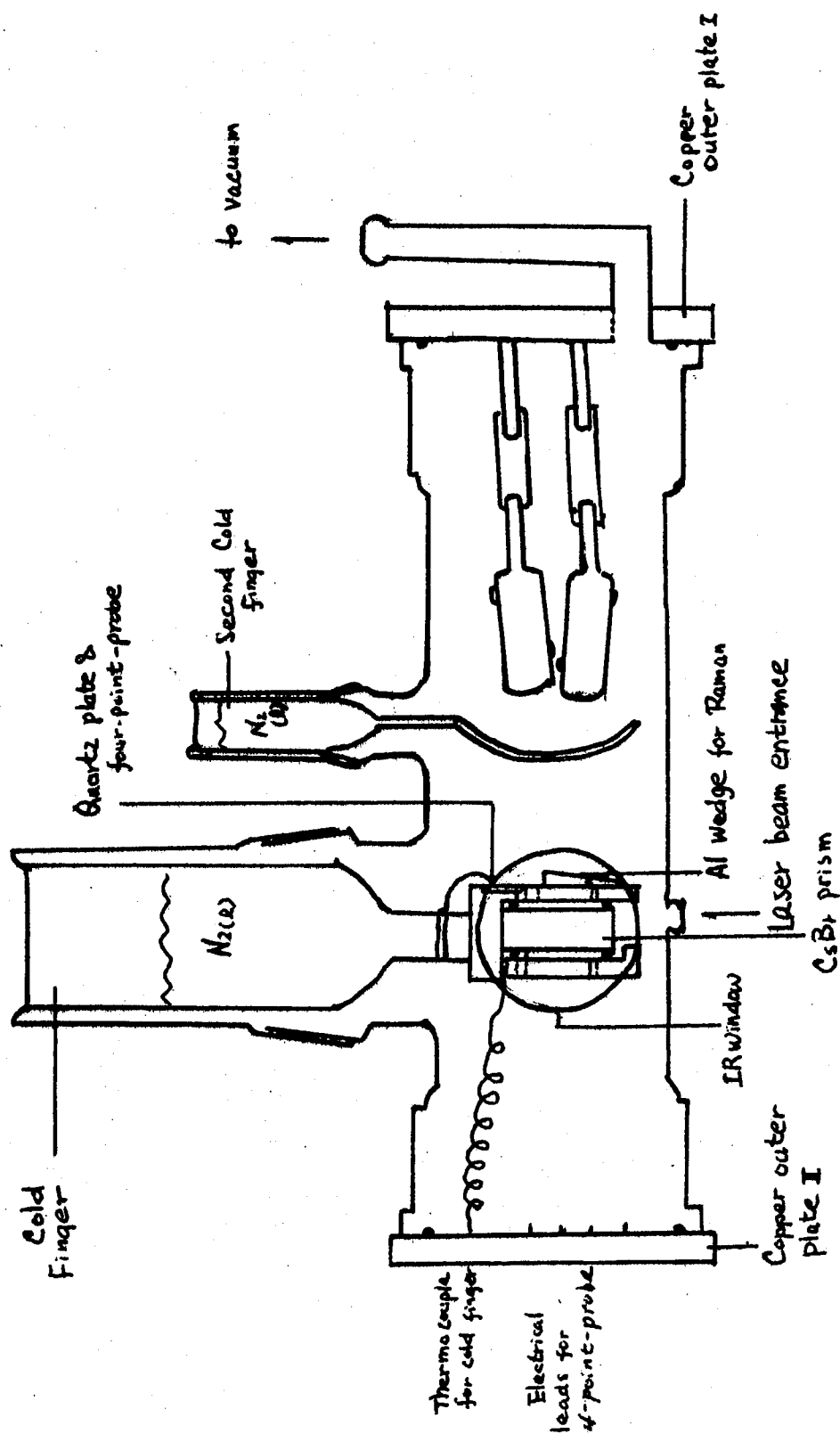
Figure 6. The Cell Body
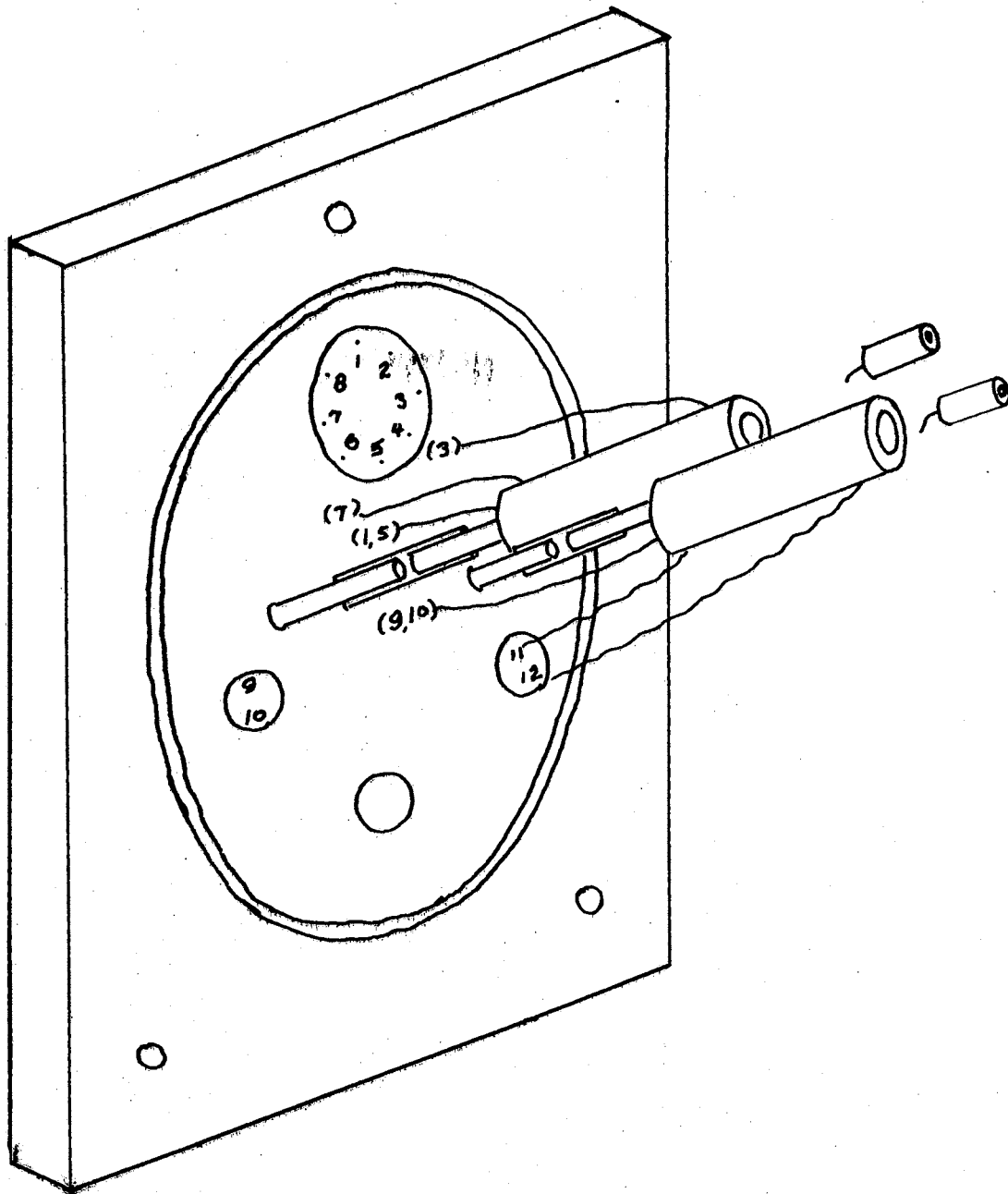
Figure 7. Copper Outer Plate I
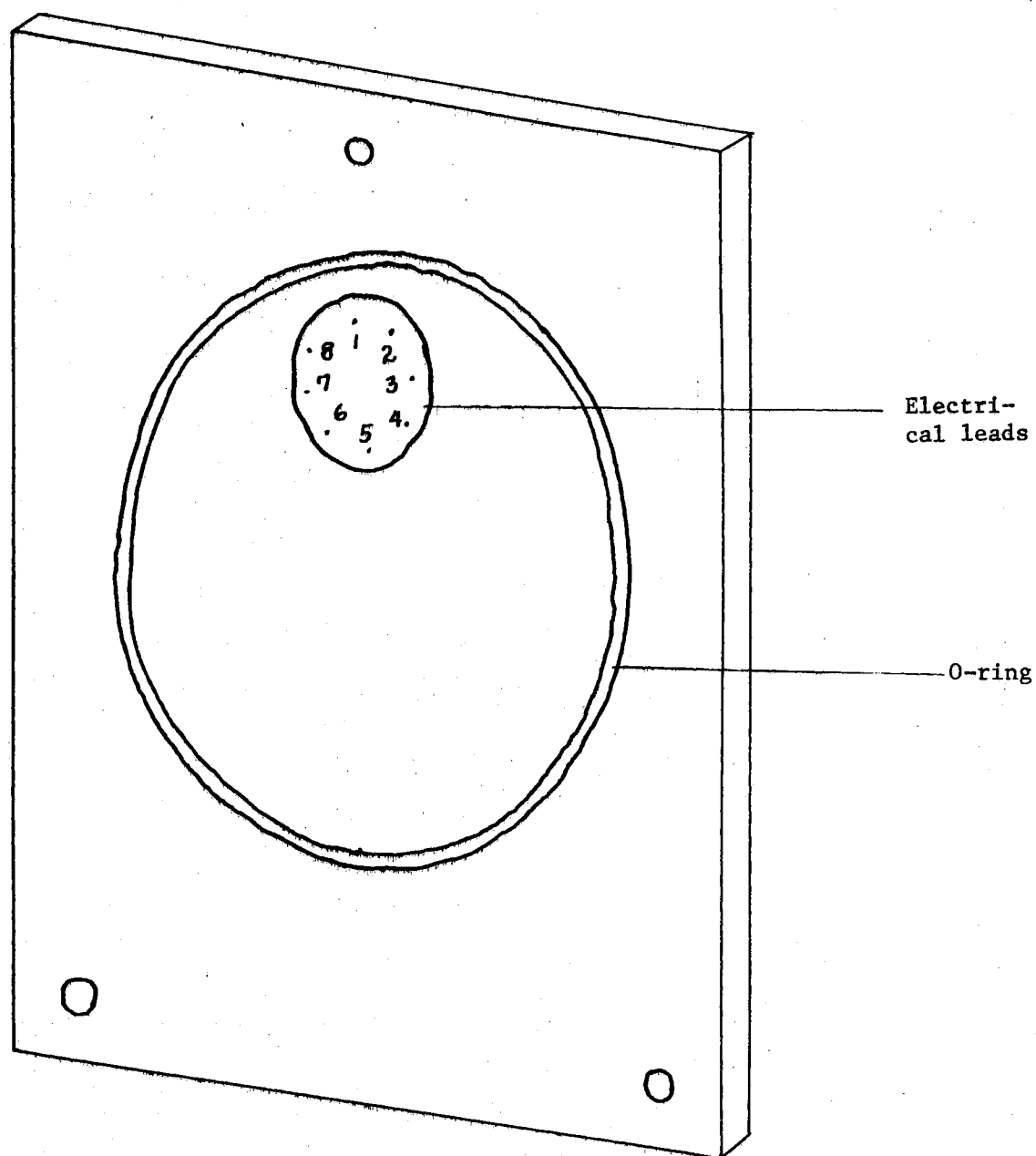
Figure 8. Copper Outer Plate II

and transferred to the vacuum line.

Sample Preparation

Since there was n-heptane in the alkali metal Knudsen cell, it was immediately pumped out and trapped. A pressure of $\sim 10^{-5}$ torr was needed to insure good deposits. The role of the beam stopper was an essential one at the beginning and after deposition had been completed. Most of the unwanted beam could be intercepted and condensed on the cold copper shield. The heater temperatures were chosen in such a way as to give the desired organic-metal concentration ratio.

Prior to sample deposition, it was necessary to heat the cryotip ($\sim 100^{\circ}$C) in order to eliminate all of the surface moisture condensed on it. Since the sample is deposited at 25°C on the substrate, such moisture is highly reactive towards the complex.

Consider a potassium-naphthalene deposition as an example, (preparation of the green complex). Potassium was heated to 215°C while naphthalene was held at about 80°C until a green color on the shield was observed and the temperatures of both ovens were quite stable, allowing smooth deposition. The shield was then turned away from the molecular beams. If the substrate is at room temperature, a uniform transparent green-colored film covered the surface of the cryotip within 90 minutes. After both heaters were turned off, the cold shield was rotated back to protect the deposit. This procedure was completed before the deposit is kinetically stabilized at reduced temperature to avoid a detectable deterioration which was observed in a few hours at room temperature, even in a 10^{-5} torr vacuum. Since the naphthalene molecules are volatile at 25°C, the preparation at that temperature guarded against the deposi-

tion of pure organic in organic-rich deposits, while potassium was suf-
ficiently mobile and reactive at 25°C to insure the absence of metal
aggregates in the metal-rich deposits. In the original experiments, the
sample was co-condensed onto a substrate at ~100°K but the occlusion of
unreacted metal or organic aggregates, though a source of some unusual
spectroscopic effects, produced some confusion in the interpretation of
optical as well as electrical measurements.

The optimum sample film thicknesses required for the infrared spectra
were, in general, too great for the observation of details in the elec-
tronic absorption spectra, though qualitative data have been obtained.
Raman spectra were also easily obtained although broad fluorescent
spectra with sharp spikes of Raman features, as a result of laser exci-
tation, have been observed in various cases. Resistivities were deduced
indirectly through the current-voltage relations. Measurements were
mostly carried out at liquid nitrogen temperature to reduce the possible
decomposition at elevated temperature even at 10^{-5} torr pressure. Several
infrared spectra were run at room temperature immediately after deposi-
tion.

Instruments and Techniques

(1) Infrared spectra of samples, observed using a Beckman IR-7
with sodium chloride prism between 600 cm^{-1} and 4000 cm^{-1}, were the most
informative data enabling one to distinguish the different samples after
many repeated investigations as the concentration ratio was adjusted
primarily by the variation of Knudsen cell temperatures of either com-
ponent. Transmission spectra, as well as atr, were easily observed with
proper sample thicknesses and transparencies. Especially, when the

sample was prepared in the optical path of the instrument, atr bands
served as a monitor of how well the complex was being formed on the
center prism. Figure 5 a illustrates how this is possible.

(2) Raman spectroscopic investigations, with argon-ion-laser 4880
$\overset{o}{A}$ (blue line) and 5145 $\overset{o}{A}$ (green line) excitation, can be used not only
to observe the ordinary Raman scattering of the complex but also to ob-
tain the resonance Raman effect for certain modes since the wavelength
of the exciting lines and the color of the sample favor this type of
phenomenon as predicted by theory. However, impurities in the organic
chemical were sometimes highly fluorescent, which obscured the observa-
tion of the Raman spectra. Comparisons with infrared spectra for a
given sample were helpful in interpreting why the fluorescence was ob-
served, e.g., excess neutral organic crystals in the sample, or sample
being thin. Presumably, certain excited states of excess neutral organic
molecules were populated by the transfer of the anion-absorbed photon
energy in the presence of the complex, with very thin samples favoring
observation of the subsequent fluorescence.

Single reflection of the laser beam with observation of the 90°
angle scattered photons from an Al wedge was the only technique employed
in obtaining both Raman spectra and fluorescent spectra. Raman spectra
of the complexes with considerable stability, e.g., 2:1 or 1:1, were ob-
served with no difficulty although slight bleaching with the laser beam
was occasionally observed with the 1:1 complex when the excess organic
chemical contained in the Knudsen cell vaporized causing a pressure in-
crease inside the whole apparatus. No useful Raman spectrum has been
observed with a sample concentration ratio of approximately 1:2 (organic
rich). Heavy bleaching of such samples by the laser beam during the

course of observations prevented one from obtaining strong Raman signals, and the fluorescence of the bleached complex gave no further valuable information.

A Jarrel-Ash 25-100 dual monochromator fitted with a ITT-FW 130 PM tube and photon counting gear was the instrumentation for both Raman scattering and the fluorescent spectroscopy (Figure 9).

The assignment of a sharp band to a Raman effect rather than sample fluorescence was based on the various observed band positions; i.e., if the observed frequencies were essentially unchanged relative to the exciting lines regardless of whether the green or the blue excitation line was used, such bands were attributed to Raman shifts, but if the observed absolute band frequencies were little or no different, emission was indicated.

(3) Qualitative electronic absorption spectra in the visible region 12 kK - 21 kK were obtained by transmission employing a single beam mode and a W-lamp for source energy. The same spectrometer was employed as in the investigation of the Raman spectra.

(4) Electrical resistivities of the various samples were measured by using a four-point-probe (55) with a probe spacing of 1/2 cm. The four probes were made of copper in contact with four strips of deposited bright gold and, thus, the sample film. A Keithley 417 picoammeter and Philbrick/Nexus milivoltmeter served for obtaining current and voltage readings respectively, and the resistivity was calculated as $\rho = 2\pi d \frac{V}{I}$, (55) with d, the probe distance; V, the observed voltage drop; I, the current in amperes and assuming a uniform sample with a film thickness small compared with the surface area.
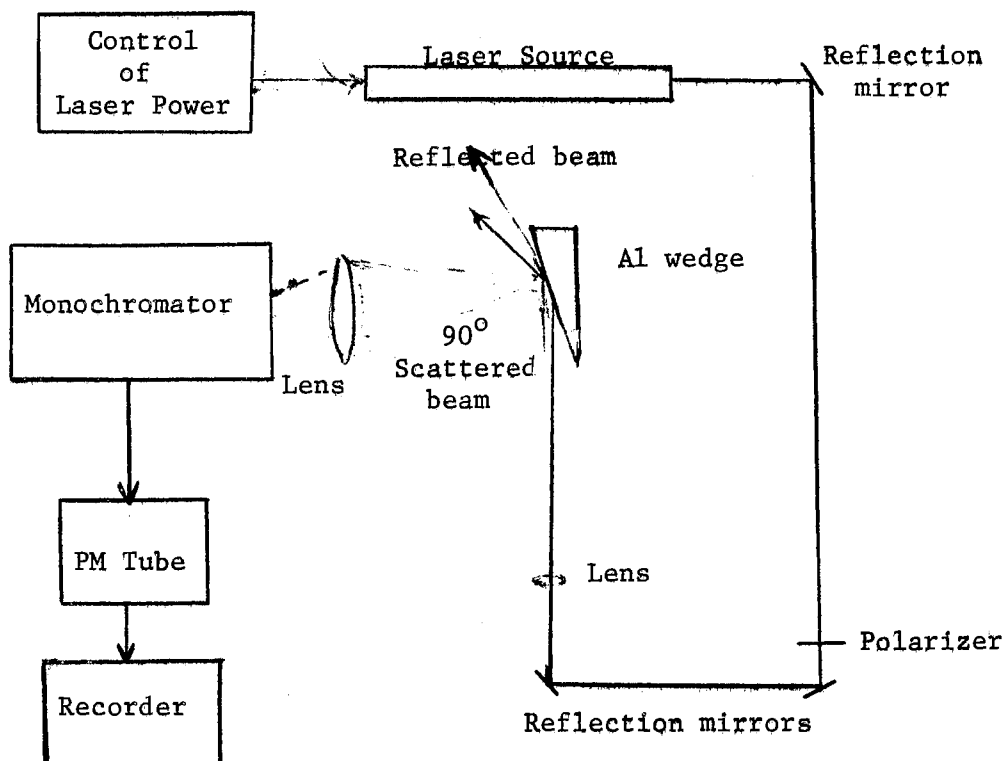
Figure 9. The Block Diagram of Raman Spectrometer

CHAPTER IV

RESULTS AND DISCUSSIONS

In contrast to the idea of the solid solutions conceived by Ubbel-
ohde (12,13,14,15,16) three distinct crystalline stoichiometric salts of
naphthalene are apparently prepared by the variation of potassium-
naphthalene beam density ratios through the control of pin hole sizes of
the Knudsen cells and deposition temperatures. The existence of the
salt crystals is evidenced by their unique vibrational spectra that dif-
fer significantly from each other as well as from that of pure naphtha-
lene. Also, strong charge-transfer interaction is suggested, since the
infrared spectra indicate that considerable dative character is involved
in metal-organic association in each case. It is proposed that the
crystalline salts of potassium-naphthalene can be described as (a) two
potassium atoms per naphthalene molecule (K_2Npt), (b) one potassium atom
per naphthalene molecule (KNpt), (c) one potassium atom per two naphtha-
lene molecules ($KNpt_2$) based on the approximate metal-organic ratios, the
consistency in observing three sets of unique and sharp vibrational
spectral features, and the variation in relative intensities with depo-
sition of one component predominantly over the other. This technique
does give a reasonably consistent result that confirms the existence of
three salts with a cation form of potassium in each case, i.e., green-
blue (K_2Npt), green (KNpt), yellow green ($K Npt_2$). However, it has not
been proven that the actual ratio of the components are 2:1, 1:1 or 1:2

44
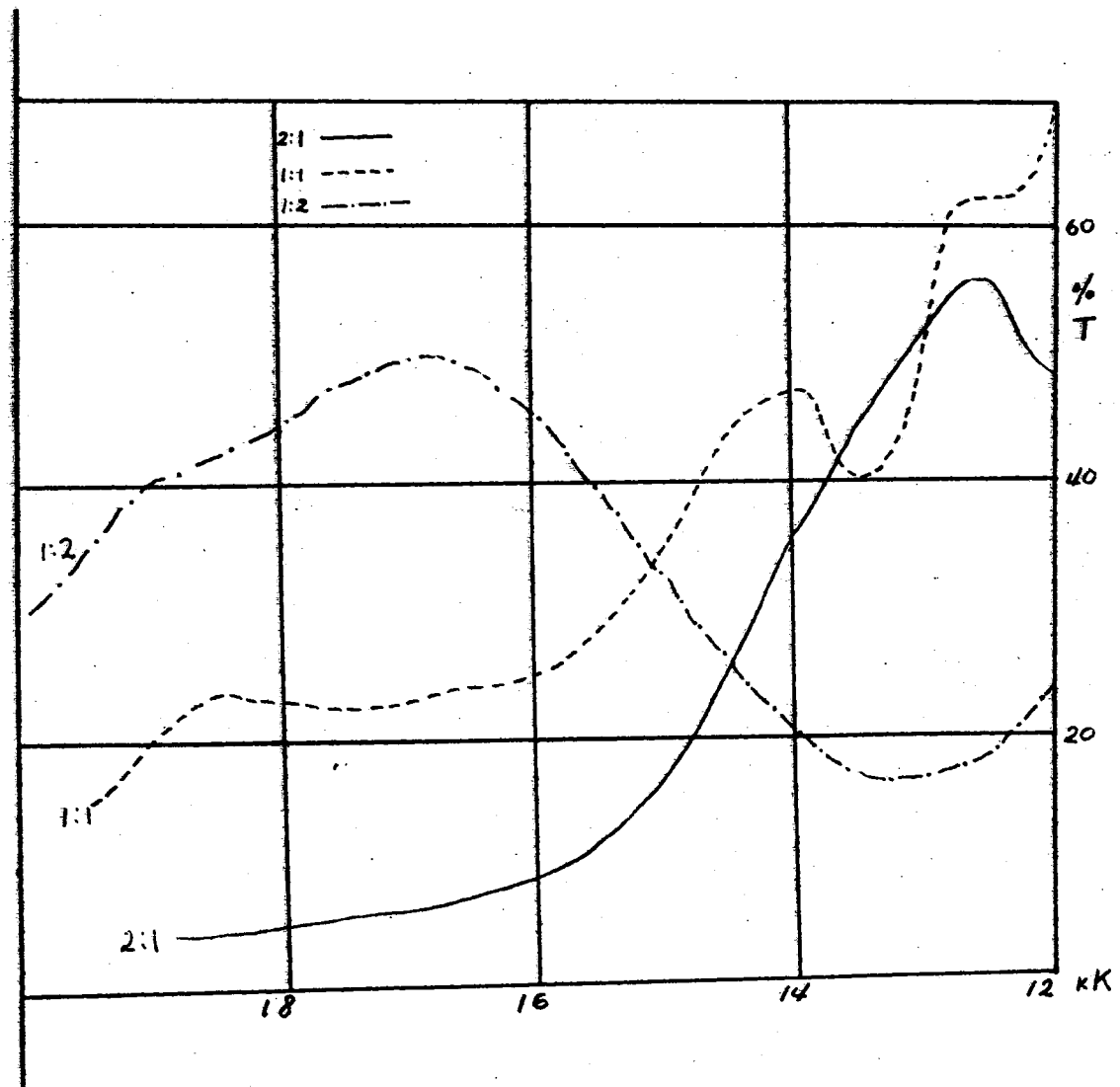
Figure 10. Electronic Absorption Spectra of K-Npt Systems

during deposition of the three salts.

Electronic Excitations in Aromatic Hydrocarbon Ions

Electronic Absorption Spectra

Qualitatively useful visible absorption spectra for potassium salts
of naphthalene are presented in Figure 10 for the frequency range 12
kK to 21 kK, the region where new bands are known to appear in the solu-
tion spectra of the mono/di-negative ions of naphthalene and mono/di-
negative ions of anthracene, but no solution data for $K A_2$ or $K Npt_2$ has
been reported.

The transitions involved are considered to be from the ground elec-
tronic state of the anion to an internal excited state of the same anion.
The electronic spectrum of KNpt salt is very similar to the solvated
mono-anion of sodium salt with band positions around 12.3 kK, 13.15 kK
and 16.2 kK. A large change of curvature near 19.5 kK also indicates
that there exists another absorption band as would be expected from the
solution spectrum.

According to Rowland and Hush (40), the anion energy states, as
predicted by simple perturbation theory, are as Tables I, II.

Hush (40) reported the electronic spectrum of the potassium salt of
monoanthracene in tetrahydrofuran showing considerable vibrational struc-
ture with energy spacing varying from 1,400 cm^{-1} to 1,800 cm^{-1}. In the
present investigation, it has been observed that there are three distinct
absorption bands at 15.7 kK, 17.1 kK and 20.7 kK in KA. Apparently, the
difference between the first two bands is 1400 cm^{-1}. This corresponds
to the Raman active vibrational mode in the KA salt excited state.

In the case of the potassium salt of naphthalene (KNpt), the ob-

TABLE I

CALCULATED Npt⁻ ENERGY STATES, CONFIGURATIONAL INTERACTION EXCLUDED,
LEVEL 1 - 5 ARE DOUBLY OCCUPIED IN NEUTRAL Npt

	No.	Hückel Energy (β)*
	2'	$- 1.618$
	3'	$- 1.303$
	4'	$- 1.000$
	5'	$- 0.618$
	5	0.618
	4	1.000
	3	1.303
	2	1.618

*$\beta = - 20.5$ kK.

TABLE II

CALCULATED A⁻ ENERGY STATES, CONFIGURATIONAL
INTERACTION EXCLUDED. LEVELS 1 - 7 ARE
DOUBLY OCCUPIED IN NEUTRAL ANTHRACENE

	No.	Hückel Energy (β)*
	3'	- 1.414
	4'	- 1.414
	5'	- 1.000
	6'	- 1.000
	7'	- 0.414
	7	0.414
	6	1.000
	5	1.000
	4	1.414
	3	1.414

*β = - 20.5 kK.

served vibrational spacing is about 1350 cm^{-1} which also corresponds to the Raman feature of the symmetric stretching mode in the 1:1 case (see Figure 13 and Table IX).

Since the donor is potassium only, a comparison of the electronic spectra between A$^-$ and Npt$^-$ can be valuable in drawing some conclusions.

(a) Considering the relative size of the π-electron cloud in each case, the interaction between the transferred electron and the π-electron cloud on the naphthalene molecule might have a more pronounced effect than on the anthracene molecule. The red shift of the first strong absorption band from anthracene mono-negative ion to the naphthalene mono-negative ion associated with the same cation agrees qualitatively well with solution data (8,9).

(b) The green color of either anion indicates that these species will have similar overall absorption bands, the complementary hue of the green color.

In the case of the di-negative ions of naphthalene (and anthracene), the orbital 5' (and 7') is occupied by two electrons. This implies that the excitation 5 - 5' (and 4 - 5') cannot take place. Hence, the corresponding transitions are 5 - 4' (and 5' - 4). The observed spectra in the solid state are different from the solution spectra. No obvious band maximum in K$_2$Npt is obtained, but strong absorption, which appears from 13 kK to 20 kK, coincides with a known absorption band of the naphthalene di-negative ion associated with Li$^+$ as observed in THF solution at room temperature (8). K$_2$A has a structured absorption band near 18 kK as does the dianion in association with potassium cation in solution (23). The spectral shifts for solution data have a systematic red shift for the di-negative ions from naphthalene to pentacene. This is also

TABLE III

COMPARISON OF ELECTRONIC ABSORPTION SPECTRA
IN SOLUTION AND SOLID STATE WITH THE
CALCULATED VALUES OF K Npt

| Band | Energy kK (Solution) | | Energy kK (Solid) this experiment |
	Observed	Calculated	
a	12.3*		12.3
	12.4**	13.995	13.65
	13.6*		16.2
			19.5
b	----	20.114	
p	----	20.432	
	31.55*	30.273	
	34.25*	35.003	

*Data from Hush and Rowland.

**Data from Hoijtink.

TABLE IV

COMPARISON OF ELECTRONIC ABSORPTION SPECTRA
IN SOLUTION AND SOLID STATE WITH
THE CALCULATED VALUES OF KA

Band	Observed (Solution) Energy in kK		Calculated Energy kK	This Exp. (Solid) Energy in kK
a	13.83*	14.0**	8.58	
p	10.81		15.385	
	12.35			
	15.00			15.75
	16.78			17.10
b	18.25	27.1	24.9	20.7
α_1	27.32	30.6	27.1	
α_2	27.32	38.8	33.0	
			41.7	

*Data from Hush and Rowland.

**Data from Hoijtink.

Hypothetical level
(neutral pair)

S_2 —————— 2nd excited singlet

S_1 —————— 1st excited singlet

Interstate crossing

T_0 —————— Triplet

Conduction level (assumed)

S_0 —————— Ground state
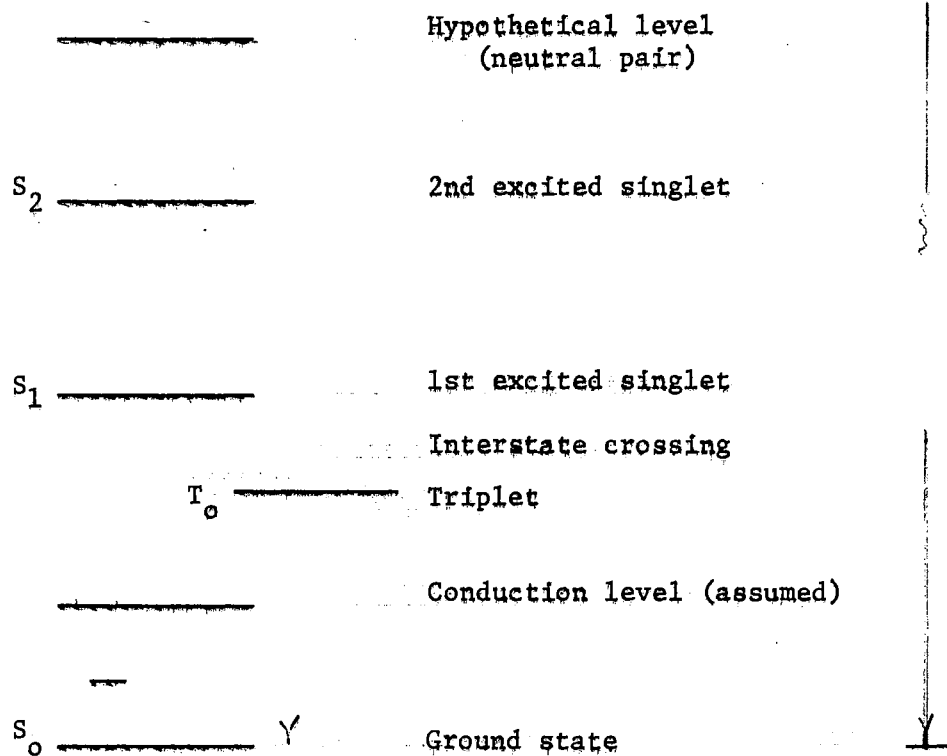
Figure 11. Energy diagram of a hypothetical CT complex

observed in solid state spectra for naphthalene and anthracene.

Comparison of KA_2 and $KNpt_2$ indicates some irregularity. There is an absorption band about 13.2 kK in $KNpt_2$, but no obvious band maxima in KA_2. There is no solution data available for comparison.

All visible region electronic transitions of the anions observed experimentally and predicted theoretically, are considered as internal transitions. No charge-transfer absorption band has been reported. A reasonable interpretation is that this transition falls in the UV region for the dative type of complexes. An energy diagram is thus presented for which $h\nu_{CT}$ falls in the UV region (see Figure 11). Therefore, it is suggested that one should extend the spectral regions in order to obtain some data concerning the value of $h\nu_{CT}$.

Emission Spectra

Fluroescence spectra observed in this investigation using argon ion laser 4880 $\overset{o}{A}$ and 5145 $\overset{o}{A}$ lines as excitation sources have not been attributed to pure anions, particularly, for mono or di-negative ions of anthracene, and possibly for mono or di-negative ions of naphthalene, since there was no fluorescence for the complexes formed between potassium and the arenes in a relatively pure state. It is, however, suspected that the fluorescence spectra of anthracene samples in the visible region is actually from the fluorescence of naphthacene impurity. Katul and Zahlan (58) reported the fluorescence spectra of naphthacene. Gorshkove (59) studied the impurity fluorescence spectra of anthracene. Very pronounced emission bands were attributed to the presence of naphthacene at 10^{-4} gram ratio, the observed fluorescence spectra of anthracene salts with excess of anthracene when excited by 4880 $\overset{o}{A}$ line re-

TABLE V

EMISSION BANDS FOR K_2Npt, K Npt AND K N pt_2 (FOR RELATIVE INTENSITIES, SEE FIGURE 12-a AND b)

K_2Npt (cm^{-1})		K Npt (cm^{-1})		K Npt$_2$ (cm^{-1})	
5145 Å Excitation	4880 Å Excitation	5145 Å Excitation	4880 Å Excitation	5145 Å Excitation	4880 Å Excitation
18838 (m)	18922 (s)		18992 (s)		
				18563 (v.v.s. sharp)	18563 (v.v.s. sharp)
	17992 (s)		17992 (s)	17963 (m)	17992 (s)
		17722 (s)		17338 (s)	17390 (v.s.)
17468 (s)			16742 (m)	16838 (m)	16992 (s.)
		16588 (m)		16208 (sh.)	16212 (sh.)
				15838 (m)	15942 (m)

s, strong; m, medium, v.s., very strong; sh. shoulder.

sembled the emission spectra of naphthacene monomer, and the fluorescence spectra of the same salt excited by 5145 $\overset{o}{A}$ line resembled the emission spectrum of the crystalline solid of naphthacene (58).

In most cases, neither pure naphthalene, nor the naphthalene salts fluoresce while excited by either green or blue laser light. The observed luminescent spectra as presented in Table V and Figure 12-a, b cannot be designated as pure K_2Npt or KNpt fluorescence. They might be interpreted as the result of emission from the neutral naphthalene molecule assisted by the presence of the KNpt anions. Life-time study of the anions excited states particularly valuable in further understanding the emission spectra. One very interesting phenomenon has been observed: Whenever one has small amount of potassium which is co-deposited with a large excess of naphthalene, then a very intense sharply structured emission band located at 18,460 cm^{-1} and 18,390 cm^{-1} is observed either by green line or by blue line excitation. It is suggested that this is the neutral naphthalene $T_1 - S_o$ transition studied by Meyer (60). The assisted emission mechanism is proposed something like

$$
\begin{bmatrix} K^+ & & Npt \\ & Npt^- & \\ Npt & & Npt \end{bmatrix} \xrightarrow{h\nu_{exciting}} K^+ \quad \begin{matrix} (Npt^-)^* & Npt \\ & \\ Npt & Npt \end{matrix} \quad \begin{matrix} \text{internal} \\ \text{transfer} \\ \text{------} \\ \text{of energy} \end{matrix}
$$

$$
\dashrightarrow \begin{bmatrix} K^+(Npt^-) & (Npt)^*_{T_1} \\ & \\ Npt & Npt \end{bmatrix} \xrightarrow{-h\nu_{ph}} \begin{bmatrix} K^+ & Npt^- & (Npt)_{S_o} \\ & Npt & Npt \end{bmatrix}
$$
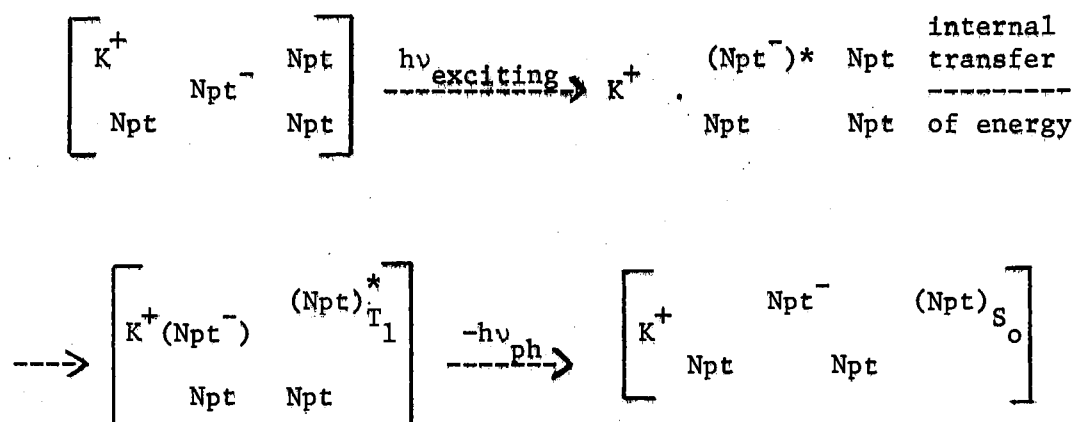
Emission spectra are normally observed by using very intense and high energy photons as an excitation source, such as produced by pulsed lasers, flash photolysis, etc. Considerable instrumentation is required
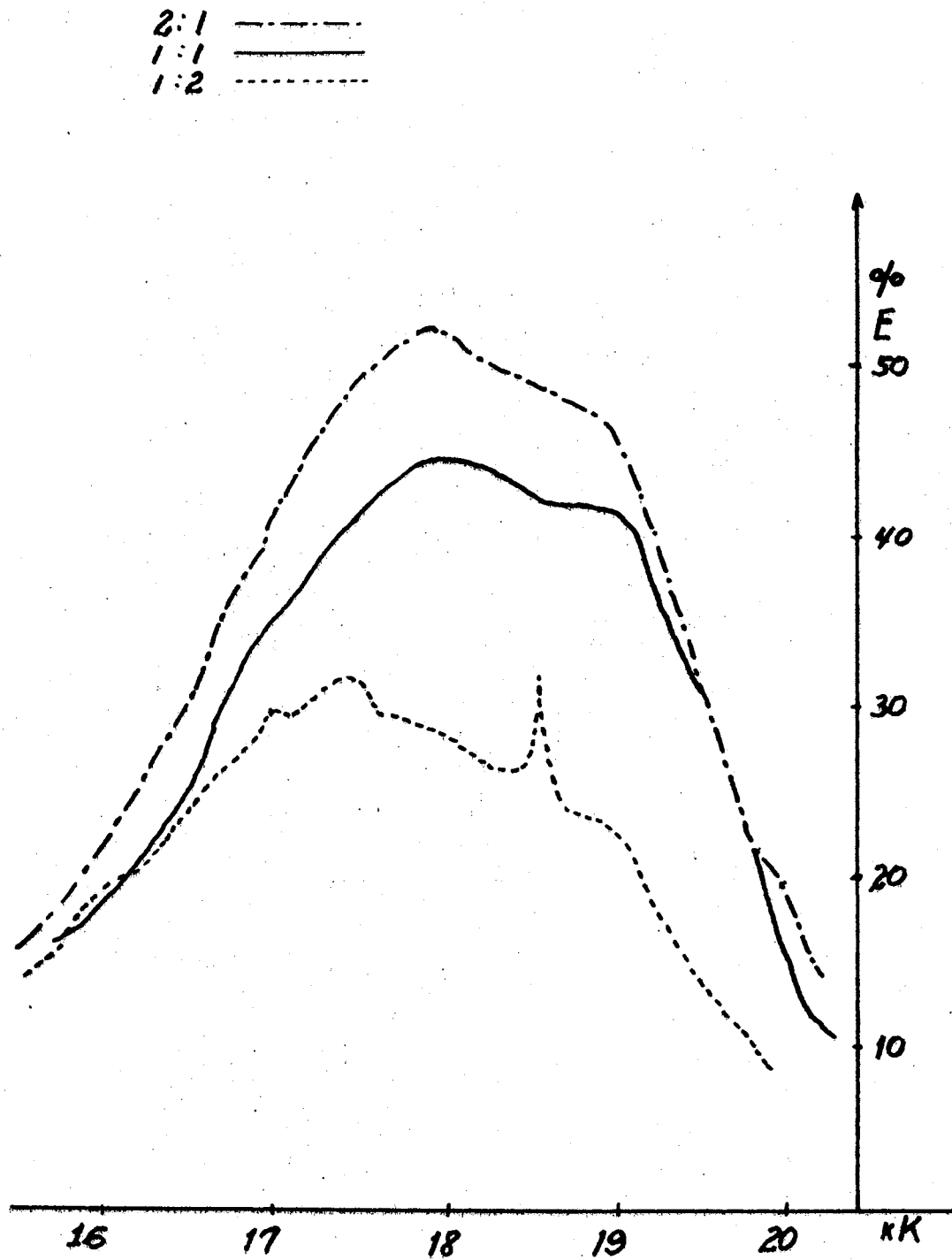
Figure 12a. Emission Spectra of K-Npt Systems Excited by 4880 Å
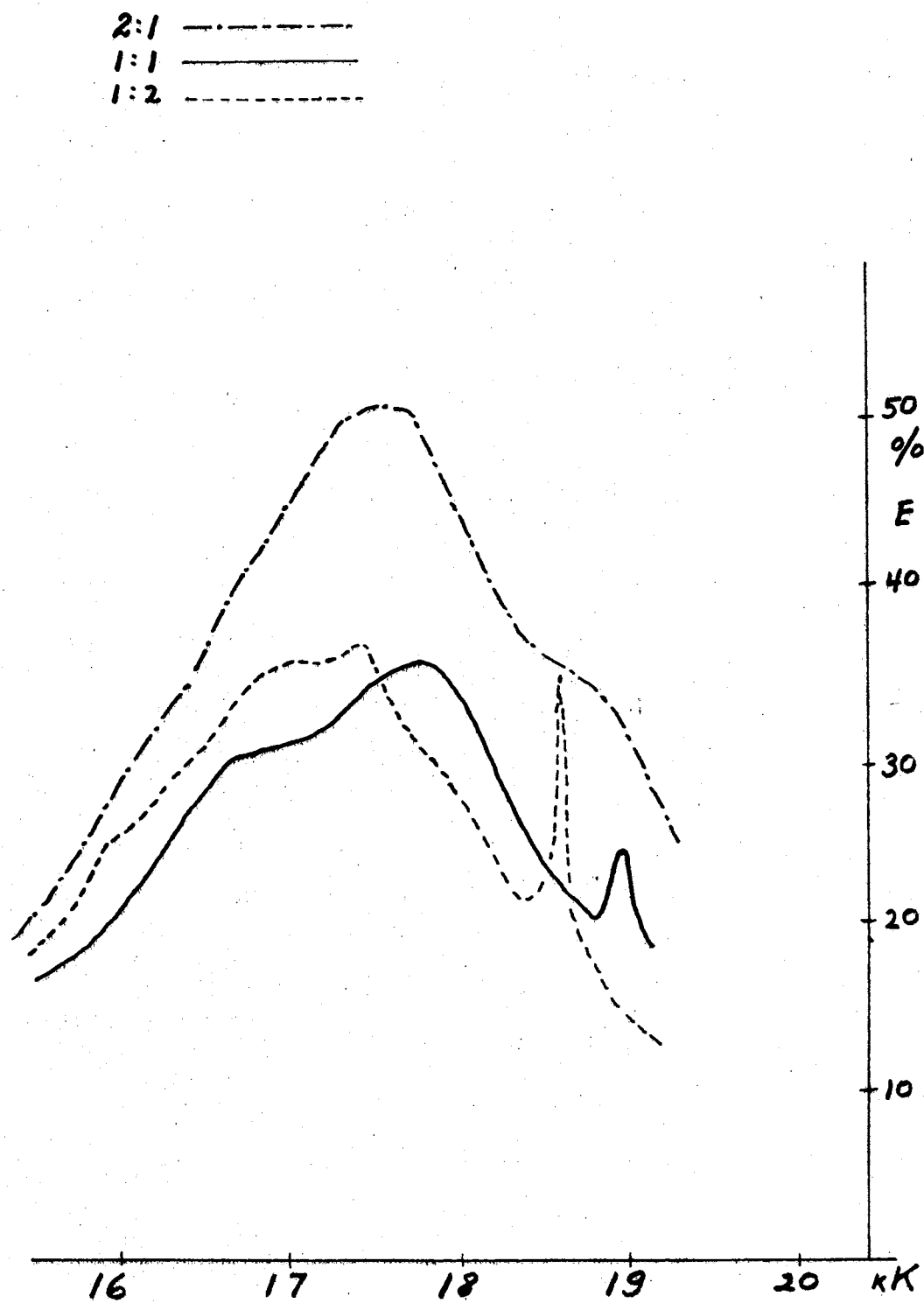
Figure 12b. Emission Spectra of K-Npt Systems Excited by
5145 Å

for these observations, but here one may have unexpectedly discovered a new technique for observing the triplet state. If so, a systematic approach for investigation of the triplet state for various arenes can be carried out by a matrix isolation technique using alkali metals as donors to induce the optical absorption.

Vibrational Spectra of K-Npt Systems

The infrared spectra for the three salts and the Raman spectra for K_2Npt and KNpt along with the spectra for pure naphthalene (bar form) are presented in Figures 13 and 14-a,b and 15. The Raman spectra are direct reproductions of original spectra, while the infrared spectrum for a particular salt, which was determined by the constant relative band intensities over a range of deposition ratios, is a composite of several runs.

Both vibrational and electronic spectra of the co-deposits clearly suggest that the naphthalene molecule can accept electrons from potassium atoms to form three distinctly different stoichiometric salts. Each salt has a unique vibrational spectrum that differs significantly from that of the pure naphthalene suggesting that considerable ionic (dative) character is involved in the metal-organic interaction in each case (29). It should be emphasized that the preparation procedures, although controlled by temperature and orifice size of the Knudsen cell, do not quarantee that one form of the salt is completely pure without the presence of theother form, because the relative densities of the molecular beams from the potassium and organic Knudsen cells have not been established with sufficient accuracy. The choice of K_2Npt and KNpt for the stable salts is fairly conclusive.
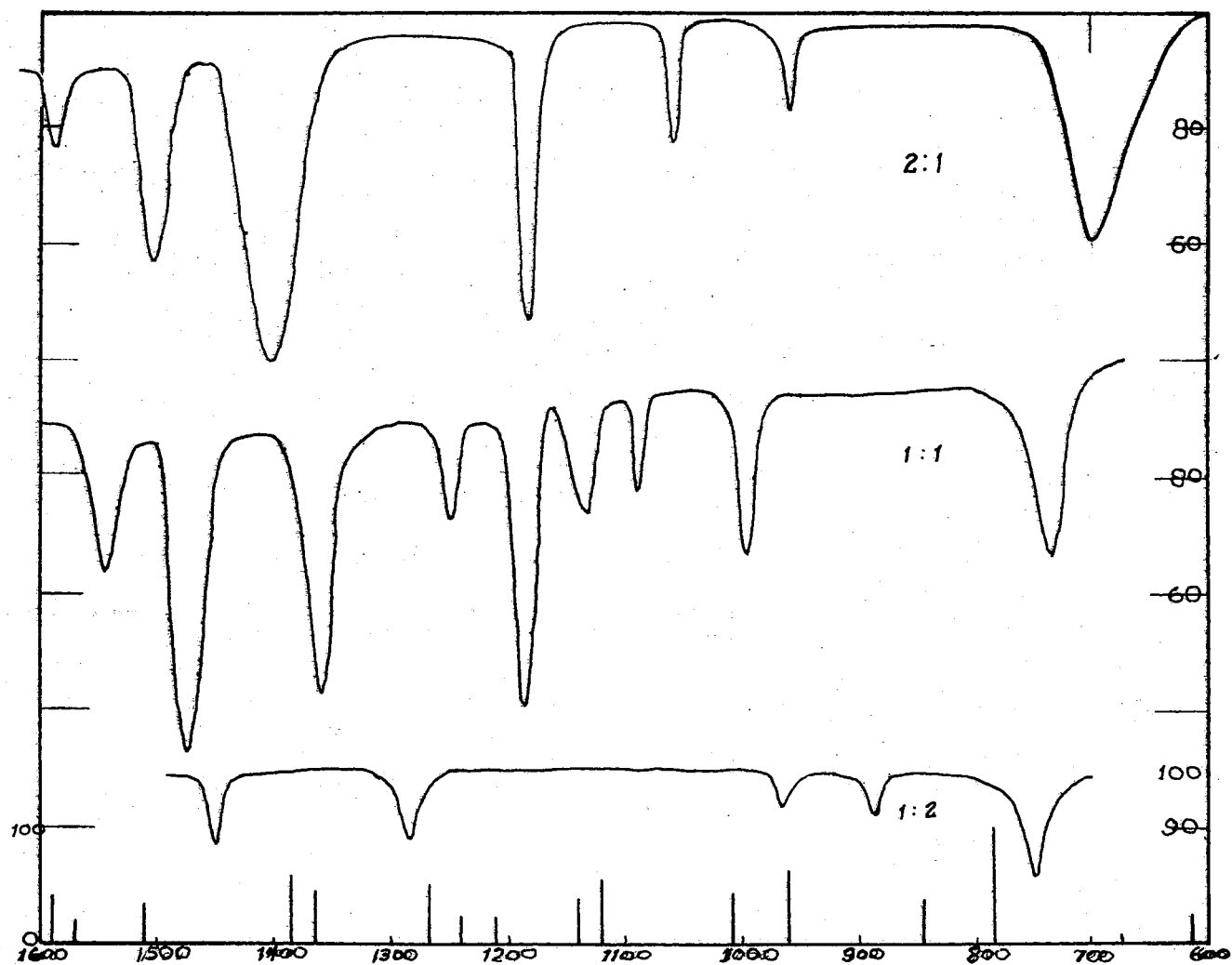
Figure 13.   Infrared Spectra of K-Npt Systems
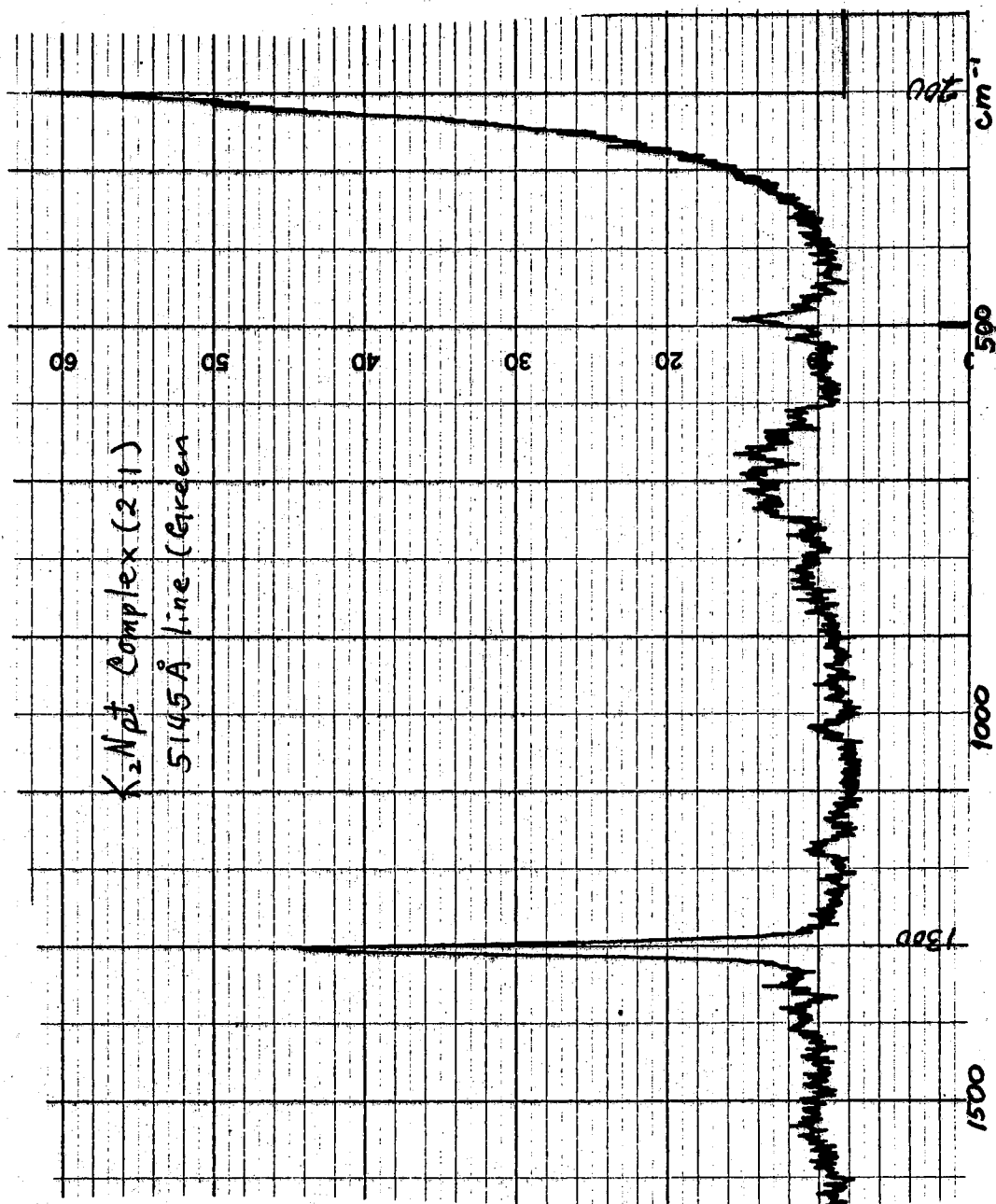
Figure 14a. Raman Spectrum of K_2Npt
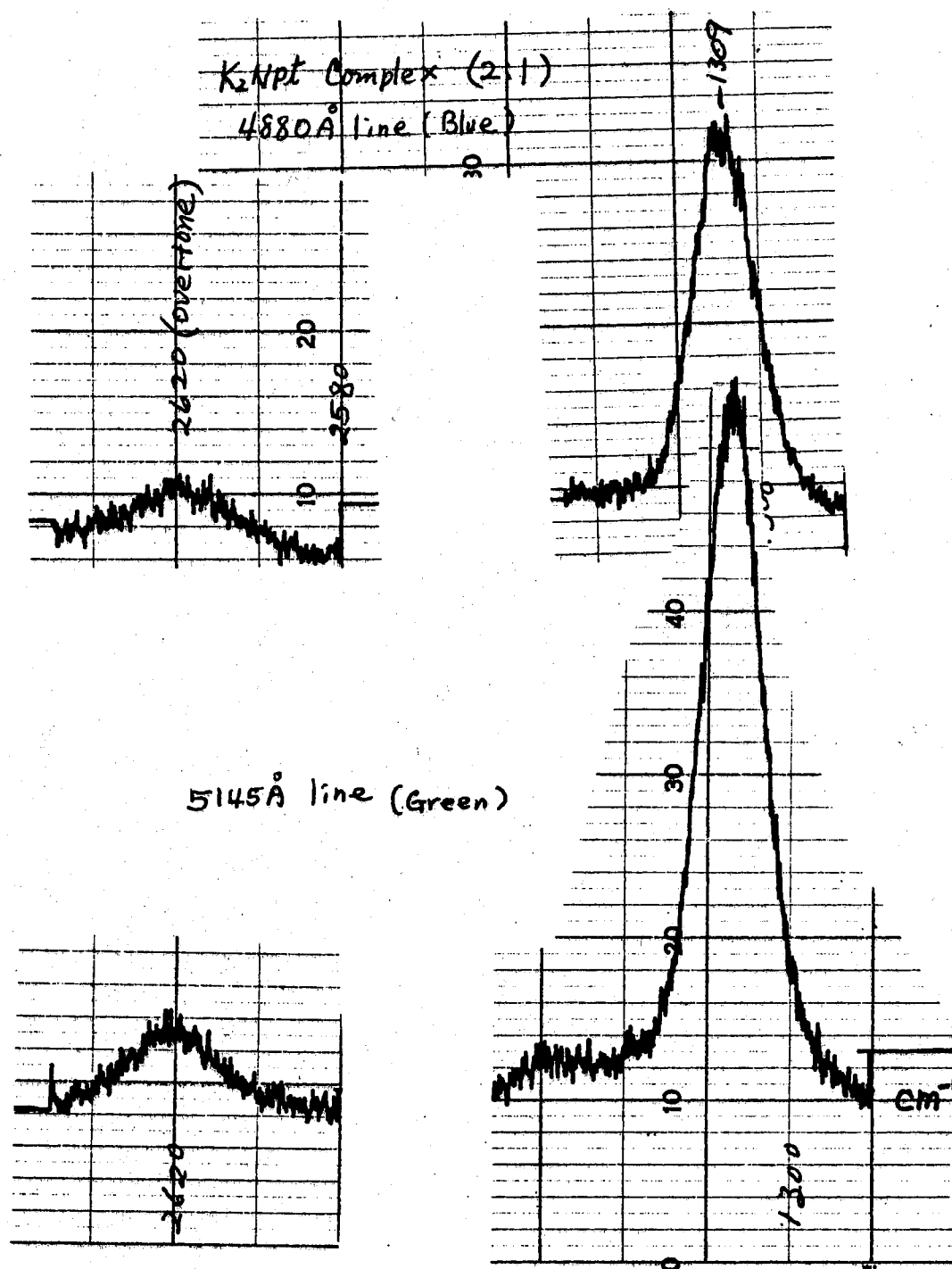
Figure 14b.   Resonance Raman Spectra of K_2Npt
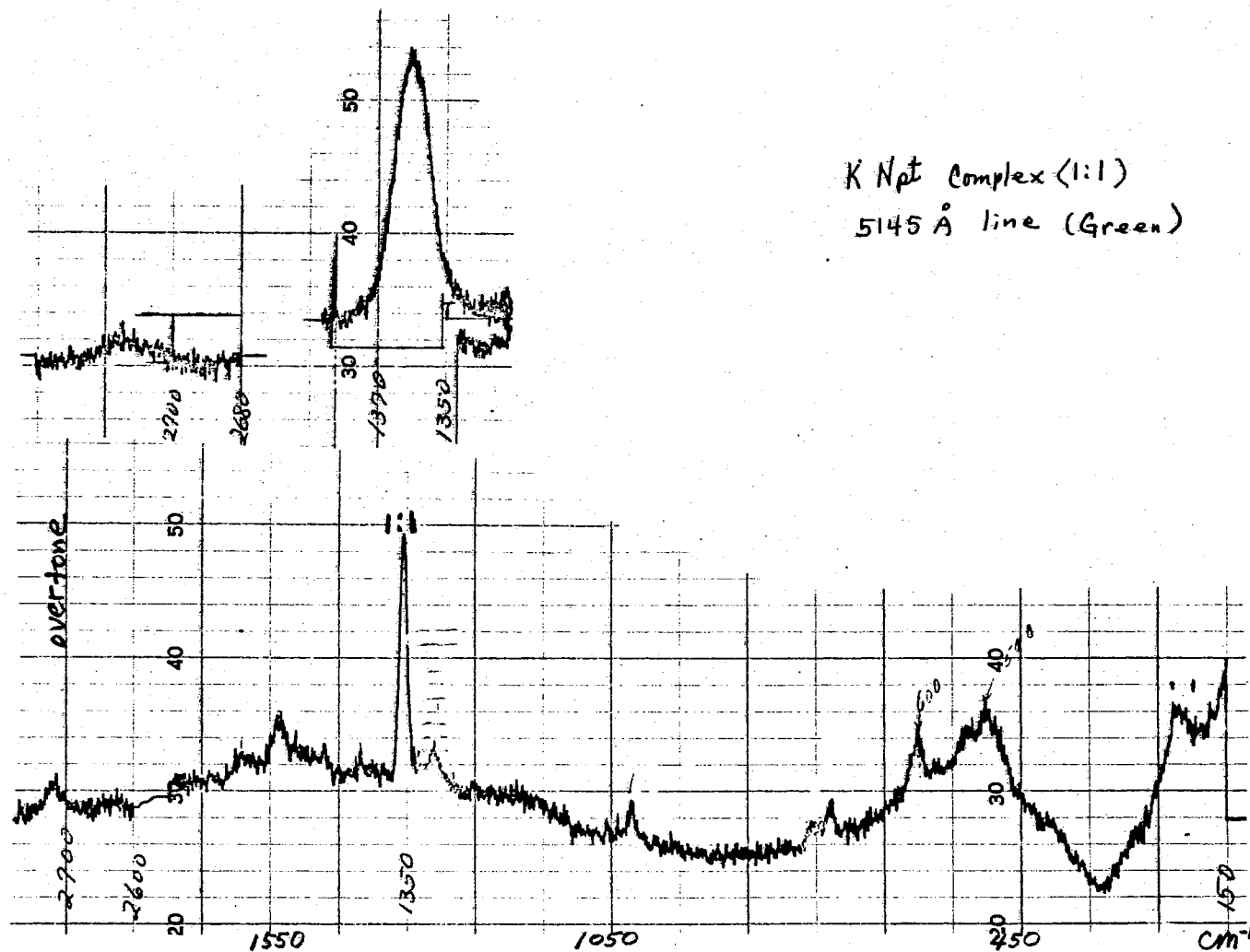
Figure 15. Raman Spectrum and Resonance Raman Spectra of KNpt

The normal modes of vibration for pure naphthalene as analyzed by Lippincott (61) are summarized in Tables VI - VIII.

TABLE VI

NORMAL VIBRATIONS OF NAPHTHALENE

Npt (D_2h) Species	No. of Vib. Mode	Activity	In-plane Or Out-of-Plane
A_g	9	R	$\|\|$
A_u	4	Inactive	$\perp$
B_{2g}	8	R	$\|\|$
B_{1u}	4	IR	$\perp$
B_{2g}	3	R	$\perp$
B_{2u}	8	IR	$\|\|$
B_{3g}	4	R	$\perp$
B_{3u}	8	IR	$\|\|$

TABLE VII

SPECTRAL REGION FOR NAPHTHALENE

Type of Vib.	Spectral Region in cm^{-1}
CH str.	2900 to 3100
CC str.	1300 to 1650
Ring breathing	900 to 1000
CH bending ($\|\|$)	1000 to 1500
CH bending ($\perp$)	700 to 1200
CC str. ($\|\|$)	< 1000
CC bending ($\perp$)	< 700

TABLE VIII

INFRARED BANDS OF POTASSIUM-NAPHTHALENE

SYSTEMS WITH ENERGY IN CM^{-1}

Pure Npt[*]	K_2Npt	K Npt	K Npt$_2$
785 792 796	695	737	750
847	----	----	887
962	960	995	973
1122 1126	1061	1090	----
1142	1150	1135	----
1242	----	1250	----
1268	1185	1185	1287
1385	1405	1360	
1505	1500	1480	1450
1590	1585	1545	----
3060	3010	----	----

It would be helpful to propose some geometric forms for the three

salts in order to explain the observed spectral results. One might as-

sume that the anions are still planar and preserve D_{2h} symmetry in the

salt crystals. The transferred odd electron is concentrated on the

atoms 1, 4, 5 and 8 for 1:1 case, and in the 2:1 complex

the two transferred electrons would prefer to occupy the same positions.

There has been no published report concerning the crystal structure of

these systems, although Hoijtink et. al (23) proposed for the solution

that the cation should be offset from the center along the longer axis

instead of directly on top of the mono-negative ions, in order to fit

the electronic absorption band intensity data as well as spectral shifts

associated with various alkali metal cations. For the present case,

speculative models in the solid state are proposed according to the idea

of ion association for 1:1, 2:1 and 1:2 complexes.
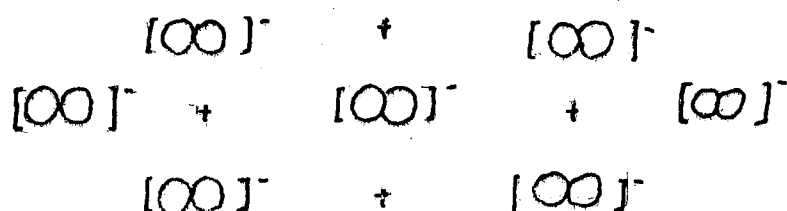
Figure 16. Possible Geometric Arrangements of 1:1
(4 Coordinated) Complex of Naphtha-
lene Anion Associated With Potassium
Cation [OO]⁻Represents the Naphtha-
lene Anion, All Lying in the Same
Plane, and Represents the Potassium
Cation, Above or Below the Anion
Plane but Offset From the Center
According to Hoijtink (22)

$$[\ooalign{}]^{2-} \quad [\ooalign{}]^{2-} \quad [\ooalign{}]^{2-} \quad [\ooalign{}]^{2}$$

$$[\ooalign{}]^{2-} \quad [\ooalign{}]^{2-}$$

$$[\ooalign{}]^{2-}$$
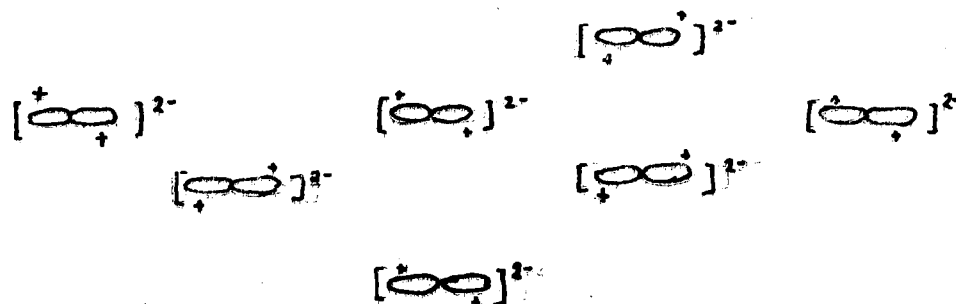
Figure 17. $[\text{OO}]^{2-}$ Represents the Side View of the Di-
negative Ion of Naphthalene, Two Potas-
sium Cations are Located One on Each Side
of the Anion Plane

$$[\ooalign{}]^{-\frac{1}{2}} \qquad (a') \qquad [\ooalign{}]^{-\frac{1}{2}}$$

$$+ \qquad [\ooalign{}]^{-\frac{1}{2}} \qquad [\ooalign{}]^{-\frac{1}{2}}$$

$$[\ooalign{}]^{-\frac{1}{2}} \qquad + \qquad (b)$$

$$(b') \qquad [\ooalign{}]^{-\frac{1}{2}} \qquad [\ooalign{}]^{-\frac{1}{2}}$$

$$(a) \qquad$$

$$[\ooalign{}]^{-\frac{1}{2}} \qquad [\ooalign{}]^{-\frac{1}{2}} \qquad +$$

$$+ \qquad [\ooalign{}]^{-\frac{1}{2}} \qquad + \qquad [\ooalign{}]^{-\frac{1}{2}}$$

$$[\ooalign{}]^{-\frac{1}{2}} \qquad [\ooalign{}]^{-\frac{1}{2}}$$
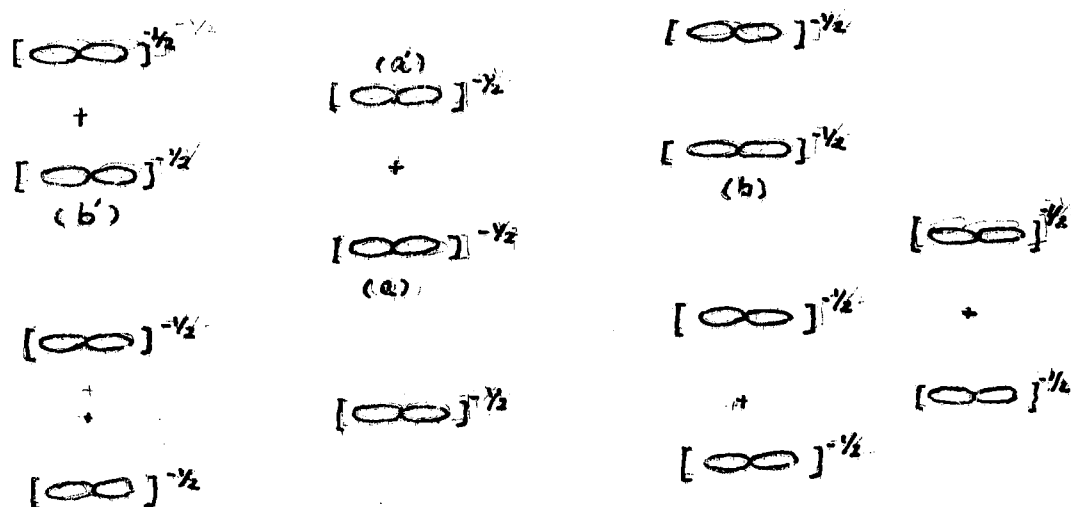
Figure 18.   Represents the Anion and Cation Arrangements in KNpt$_2$

Infrared Spectra of Solid Complexes of Potas-

sium-Naphthalene

According to the proposed models, the infrared spectra of the alka-
li-metal arene complexes may be anticipated to be very different from
the neutral arenes. Because of the dative type of the complexes, there
will result a spectrum corresponding to an anion or a di-anion (62). The
observed spectra clearly suggest that potassium-naphthalene complexes

fall in this category. Consequently, a close examination of the vibra-
tional spectra may provide a reliable method of characterizing the nature
of the anion bonding.

Our experimental observations indicate changes in frequency and in
intensity. In order to relate these changes to bonding in the acceptor
molecule, it is necessary to consider the redistribution of charge on
the acceptor molecule upon complex formation, i.e., the K_2Npt and K Npt.
Vibrations with no resulting dipole moment change in naphthalene may
suddenly appear with rather large dipole moment changes in the naphtha-
lene anions. This might give rise to the very large changes in the ap-
pearance of the spectrum. The changes in the vibrational band frequen-
cies after complexation may be related to the changes of bond orders as
a result of one or two electron-transfer. Although the transferred
electrons occupy an anti-bonding molecular orbital in naphthalene, a
systematic frequency decrease of the anion vibrations relative to the
neutral molecule is not expected according to the theoretical bond order
calculation using one electron LCAOMO approximation by Hoijtink (8,9).
In fact, one does observe blue shifts in certain vibrational modes in
the infrared as well as in the Raman spectra (see Tables VIII and IX).
These experimental spectral data would be useful for reliable anion iden-
tifications in the future and provide an empirical basis for the force
constant calculation of certain polycyclic aromatic anions.

The vibrational spectra of the potassium salts of naphthalene, as
presented in Figure 13 are quite different from that of neutral naph-
thalene. Instead of the normal B_{1u} C-H out-of-plane bending motion of
naphthalene near 785 cm^{-1}, strong absorption bands are observed with red
frequency shifts of about 90 cm^{-1}, 48 cm^{-1} and 35 cm^{-1} for 2:1, 1:1 and

1:2 complexes respectively. This seems to be the only systematic frequency change in the infrared region and gives some experimental evidence to support the anti-bonding character of the transferred electrons.

The smaller frequency shifts in 2:1 complex as compared with 1:1 complex for B_{2u} C-C in-plane stretching mode near 1590 cm^{-1} and for B_{3u} C-C in-plane stretching mode near 1505 cm^{-1} can be explained by using speculative models (Figures 16-18). In the 2:1 complex the cations are assumed to be located on each side of the molecular plane (Figure 17). If the transferred electrons are to be most densely distributed at the positions predicted by the theory, the overall effect might be large enough to cause a greater shift. However, because of the presence of the associated cations, the density of the transferred electron in certain bonds might be partially reduced thus decreasing the frequency shift. In the case of the 1:1 complex (Figure 16), there is no counterpart of the coulombic force on the other side of the anion plane, and the charge cloud on the anion cannot be regarded as a point charge. Therefore, the distribution of the charge cloud of the transferred electron which changes the vibrational frequency of certain modes might have more pronounced net effect in 1:1 case than in 2:1 case. A similar argument may apply to the shift observed for the 1385 cm^{-1} band.

The possibility of the activation of certain totally symmetric modes in the infrared spectrum of the 1:1 complex should be considered. The proposed model provides some qualitative explanation for the activation of these infrared inactive modes. Consider the observed strong infrared absorption band at 1360 cm^{-1} (Figure 13 and Table VIII) of the 1:1 complex. This band can be assigned either to the B_{2u} C-C in-plane stretching mode (1389 cm^{-1}) or to the A_g C-C (61) in-plane stretching mode (1385 cm^{-1}) of the uncomplexed naphthalene molecule.

If the A_g (1385 cm^{-1}) C-C stretching mode is to be activated in the infrared region for 1:1 complex, there must be some oscillating dipole moment associated with the vibration produced by the vibrationaly modulated polarization of the π-electron cloud by the cation (i.e., by the electron vibration mechanism) if the D_{2h} symmetry of the neutral naphthalene is preserved in the naphthalene monoanion. This mechanism as well as the cation effect on frequencies have been shown to support the activation of TCNE infrared inactive modes in the K TCNE system (27,28). The most direct approach to test this possibility would involve a Raman measurement of the A_g C-C in-plane stretching mode for the mono-negative ion. The band of the complexed salt is observed in the Raman spectrum for the 1:1 case at 1359 cm^{-1} (Figure 15 and Table IX). This is an experimental indication that the enhancement of the infrared inactive mode near 1385 cm^{-1} is a possibility. Further experimental evidence (such as the cation effect) must be sought to confirm this possibility.

In the 2:1 complex, the net induced dipole transition moment, associated with the perturbation by the two oppositely located cations, might be symmetry cancelled (Figure 17). Perhaps for this reason no infrared band could be observed in the 1200 cm^{-1} to 1400 cm^{-1} region for the 2:1 complex (see Figure 13).

Turning to the 1:2 complex, there might be some vibronic washout of ir intensity in certain regions due to the proposed structure which satisfies the condition of a caged electron as proposed earlier (28). A considerably simplified spectrum has been obtained that provides some evidence of such an occurrence in the 1:2 complex. The basic difference of the proposed models between 1:2 and 1:1 complexes is that the radical electron cloud in the 1:2 complex is essentially distributed over two

naphthalene molecules (a and a', see Figure 18), forming, with the other

two neighboring $Npt^{\frac{1}{2}-}$ (b and b') molecules, a cage for the electron.

But in the 1:1 complex the electron is assumed to localize mainly on one

anion. Although a cage could be assumed, the effect might not be to

cancel the transition dipole moment in KNpt system in certain vibration-

al modes as contrasted with the $KNpt_2$ system. More experimental as well

as theoretical work is required to clarify the results interpreted in the

previous paragraphs. The influence of cation electron affinity on cer-

tain vibrational frequencies of the various anions of naphthalene should

be a valuable experimental approach to provide more confirmative results.

The Raman Spectra of the Solid Complexes of

Potassium-Naphthalene

The A_g in-plane skeletal distortion mode near 510 cm^{-1} is observed

with red shifts of about 10 cm^{-1}, 24 cm^{-1}, and 85 cm^{-1} corresponding to

2:1, 1:1 and 1:2 complexes respectively. The bond order change cannot

be directly correlated with the observed frequency shifts for this vi-

brational mode. Similar behavior of several other bands is also ob-

served. They are tabulated in Table IX. The 1385 cm^{-1} band will be in-

terpreted in the next section. Figures 14-a, b and 15 contains the un-

touched Raman spectra of 1:1 and 2:1 complexes. No Raman spectrum for

the 1:2 case is shown although a few band frequencies are listed in

Table IX. This reflects the instability of the 1:2 salt, particularly

when it is exposed to the laser beam. It is always bleached by the in-

tense laser light even at considerably reduced power.

TABLE IX

RAMAN BANDS OF POTASSIUM-NAPHTHALENE SYSTEMS (FOR RELATIVE
BAND INTENSITIES, SEE FIGURE 15) IN CM^{-1}

Npt	K_2Npt	K Npt	$K\ Npt_2$
285	287		
510	500	486	425
	565	525	516
		600	
764	785	734	
	838		
1026	1028	976	
1145	1182	1132	1235
1384	1309	1359	1284
1465	1413		1447
1579	1587	1530	1475
	2343	2717	
	2370		
	2622		

Resonance Raman Spectra of K_2Npt and KNpt Systems

As has been indicated in Chapter II, when the exciting light enters the electronic absorption region of the sample, the resonance Raman spectra can be observed. The colored quality of potassium salts of naphthalene and the nature of the Raman sampling procedures, with the choice of a suitable exciting frequency, favored the observation of the resonance Raman effect. A proper sample thickness is required in order to avoid (1) reabsorption of the resonantly scattered light, typical in the case of bulky samples and (2) fluorescence in the case of very thin samples, especially for the mixtures rich in organic but doped with little potassium. Moreover, photolysis may occur in the course of investigation which not only destroys the sample but also produces unknown substances which strongly affect the spectral features. These difficulties may be overcome by careful sample preparation to reduce the impurities if the emission is caused by impurities, or choosing lower excitation frequencies, if emission of photons is a property of the sample, or using considerably reduced power of the exciting line. It has been found that both K_2Npt and KNpt show the resonance Raman phenomenon, particularly with green line (5145 Å) excitation.

In the uncomplexed naphthalene molecule, the totally symmetric C-C stretching mode is Raman active at 1385 cm^{-1}. This band position is shifted to 1359 cm^{-1} in KNpt and to 1309 cm^{-1} in K_2Npt, which qualitatively agrees with the predicted bond order change. The anti-bonding character of the transferred electrons can be understood in terms of the Raman frequency change of the C-C stretching mode. Although this mode in K_2Npt also shows a resonance effect with blue line (4880 Å) excita-

tion, a reduction of intensity is observed using the blue line. The qualitatively useful electronic spectra in the visible region of K_2Npt and KNpt which have been presented in Figure 10 indicate that vibrational energy spacing of about 1350 cm^{-1} in the 1:1 complex and possibly about 1300 cm^{-1} in the 2:1 complex are involved in the electronic transition responsible for the resonance Raman effect.

The spectral features of the resonance Raman effect of the solid are a high scattering intensity which may be greater by several orders of magnitude than observed under the ordinary Raman effect. The totally symmetric stretching vibration of mono/di-negative ions of naphthalene also produces an observable overtone intensity when excited by a linear line which lies inside the electronic absorption band of the anions. Examples in observing the higher orders of overtones for I_3^- ions in various organic solvents have been reported by Bernstein (63) and Kaya et al. (64) using ultraviolet laser excitation. They concluded that for rigorous resonance Raman effect the appearance of higher orders of overtones is limited only to totally symmetric vibrations as predicted by Nafie et al. (65). In the spectra observed for the 1:1 and 2:1 complexes the resonance effect is clearly demonstrated by the presence of a strong band at 1359 cm^{-1} in 1:1 case and at 1309 cm^{-1} in 2:1 case which correspond to 1385 cm^{-1} in the uncomplexed naphthalene molecule. This mode displayed a factor of 5 greater intensity in 1:1 case and a factor of 10 greater intensity in 2:1 case than any other KNpt and K_2Npt features respectively when 5145 $\overset{o}{A}$ was used. In general, the Raman band intensities in the resonance region are strongly dependent on the position of the exciting frequency relative to the electronic absorption band maxima of the molecule.

One can further understand that in K_2Npt salt, the intensity difference with excitation frequency is caused by the fact that one of the 1309 cm^{-1} vibronic bands is near resonance with blue line excitation and in rigorous resonance with the green line excitation. The resonant character of the scattering was further evidenced by a significant overtone intensity in 2:1 complexes regardless of which excitation line was used, but in KNpt complex, the resonance effect is observed only with green line excitation as shown by the overtone band near 2717 cm^{-1} about twice the frequency of the 1359 cm^{-1} band.

Electrical Resistivities

The measured resistivities at ~100 $^{\circ}K$ listed in Table X were the average of several runs for each system under study. A laboratory D.C. source of about 15 - 30 volts was used. The circuit is sketched in Figure 5 c. At the beginning of co-condensation, no current could be detected. When sufficient amount of sample uniformly covered the whole area of the quartz plate as well as the Raman wedge and the center prism, there developed a detectable current of about 5.8 x 10^{-10} amperes, and a voltage drop of about 4.8 x 10^{-4} volt for 1:1 KA system. Specific resistivities of all samples examined in this study, were found to be in the range of 10^{-3} ohm cm for the thick potassium rich samples to 10^8 ohm cm for organic rich samples. Although temperature dependence of resistivity has been established for various alkali metal-arene systems by Ubbelohde (12), the electrical conduction might not be intrinsic due to the imperfection of the crystal and non-stoichiometry. The marked activation energies and much higher resistivities as reported by Ubbelohde (12), might be due to the intergranular resistance and electrode-sample con-

tact resistance in his experiments. Moreover, their measurements were carried out under nitrogen atmosphere, so the numerous voids among the pressed polycrystalline sample would be occupied by the nitrogen gas. With nitrogen molecules adsorbed on the bulk samples, this might be the cause of the observed large value of the resistivity. However, the thin film resistivities obtained in this study were measured with a four-point-probe in high vacuum. The values reported in Table X were calibrated with Valdes (56) curve.

The markedly enhanced conductivity in potassium-anthracene charge-transfer complexes (resistivity 10^7 ohm cm) as compared with the pure anthracene crystals (resistivity 10^{15} ohm cm) along with the spectroscopic observations suggest that these complexes are formed by strong interaction between the donor and the acceptor with nearly complete transfer of an electron from potassium atom to the anthracene molecule. That is, the ground state is dative in nature.

Structurally, the alkali metal-arene complexes might be viewed as layered type of compounds (A), i.e., systems in which donor atoms and acceptor molecules are each contained in parallel planes which are then alternately stacked together. This arrangement is realized in the proposed speculative model, for example, the 1:1 complex in Figure 16.

In Figure 4c, a solid radical salt, the electron can pass directly (broken line) into the corresponding level of the next molecule. One may modify the diagram in the presence of an electric field as well as in the presence of the associated cation
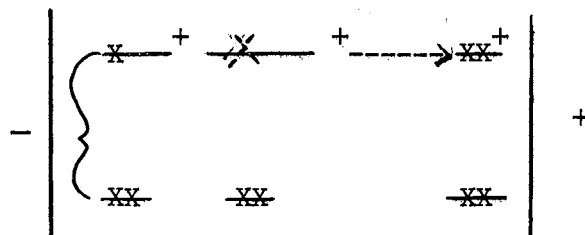
Le Blanc (B) points out that cation polarizability is the likely

TABLE X

RESISTIVITIES OF VARIOUS ALKALI-METAL ARENE SYSTEMS

Donor	Acceptor	D/A[a]	Color	ρ_o(ave.) ohm cm	$\rho=\rho_o/G_7$* ohm cm
Na	Naphthalene		violet	5.0×10^5	5.0×10^4 [b]
K	Naphthalene	2:1[e]	blue	10^7	10^6 [d]
Na	Naphthalene	1:1[e]	red	4.5×10^8	4.5×10^7 [b]
K	Naphthalene	1:1[e]	green	10^9	10^8 [d]
K	Naphthalene	1:2[c]	yellow green	10^{10}	10^9 [d]
K[f]	Anthracene	2:1[e]	blue	1.88×10^7	1.88×10^6 [d]
K	Anthracene	1:1[e]	green	1.2×10^8	1.2×10^7 [d]

*The correction factor from reference (55)

[a] Estimated from vapor pressure of D and A or via spectroscopic observation.

[b] Sample condensed at about $100°K$.

[c] Spectroscopic determined ratio.

[d] Sample condensed at room temperature.

[e] Estimated from vapor pressure equation

$$\log P = - \left(\frac{5263}{T}\right) + 12.368$$

for anthracene.

[f] Resistivity dropped sharply 10^{-4} to 10^{-3} ohm-cm when sample became thick if condensed at low temperature.

cause of the high conductivity of the TCNQ salts. By analogy, it may be the cation (in this case, potassium K^+) polarizability which causes the fairly high conductivity of the anion salts, (e.g., anthracene salts of potassium). Let one electron be moved from an anthracene anion to another one, thus carrying current. This results in a neutral anthracene molecule plus a doubly charged anthracene anion. The coulombic repulsion between the two electrons on this ion may be overcome, however, by the polarization energy of the cation. Since the anion radical is highly polarized by the point cation, only a very small amount of energy of activation may be required to cause the electron to tunnel through the intermolecular energy barrier.

Basically, the following objectives of this experimental investigation have been substantiated via an extensive spectroscopic observation. First, there are three distinctly different stoichiometric salt-like charge-transfer complexes (alkali-metal-arenes); i.e., 2:1, 1:1 and 1:2 which can be prepared from gas phase co-condensation by the variation of the metal-organic ratios; second, the existence of these complexes have been evidenced by the vibrational spectroscopic observation since both infrared and Raman spectra provide the unique spectral features which are considerably different from the pure arene molecules; third, qualitatively useful electronic absorption spectra in the visible region have also been obtained for the comparison with solution data and, to support the vibronic effect involved in the observation of the resonance Raman effect of the charge-transfer complexes; fourth, electrical resistivities at low temperature are considered to be more valuable, as compared with earlier investigators' work, because the techniques employed in sampling as well as in measuring are more reliable than previously; fifth, the colored nature of the samples as well as the Raman sampling techniques favored the observation of the resonance Raman effect.
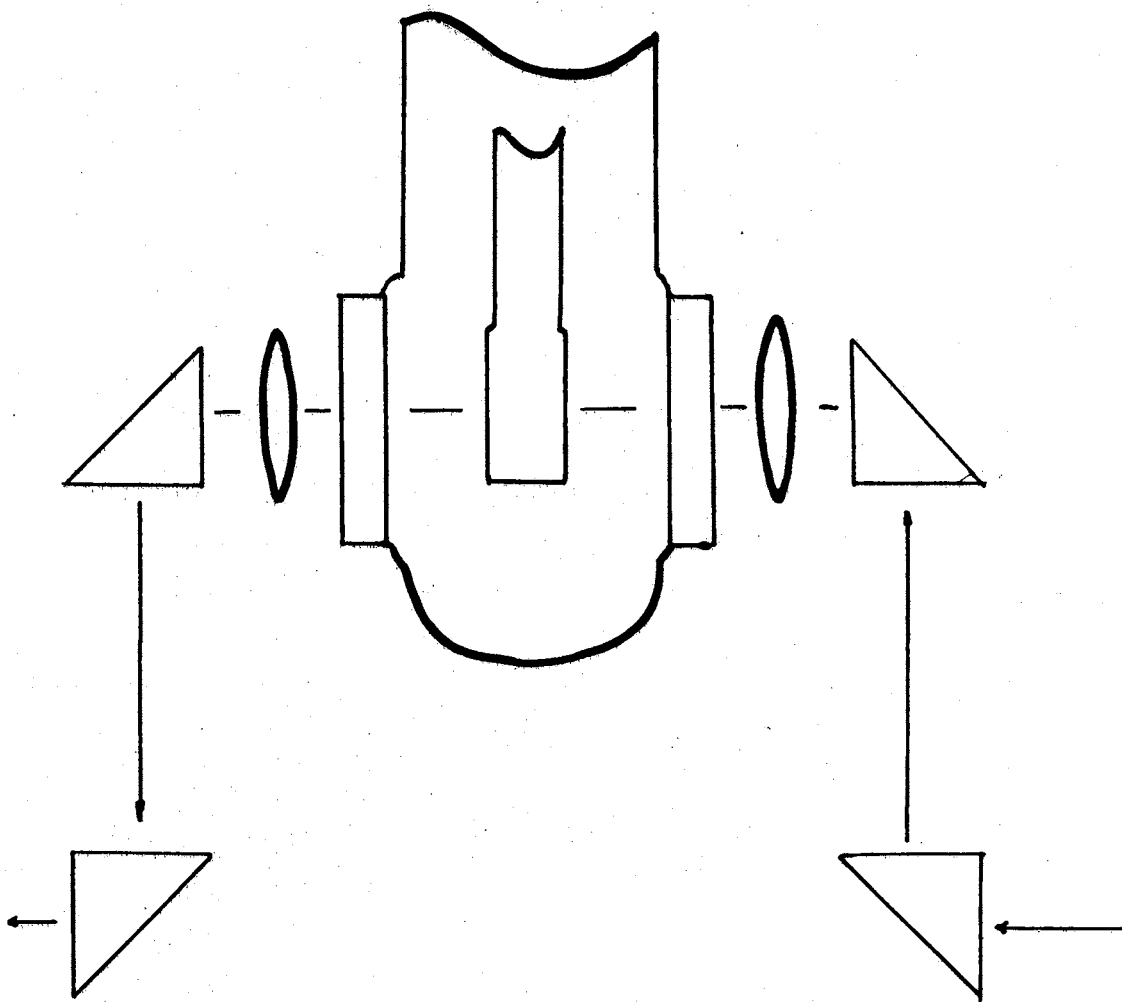
Figure 19. Suggested Optical Arrangement to Bring the Beam
Out From a Cary 14 Spectrophotometer

Suggestions for Future Work

There are several points concerning the optical properties that should be emphasized in order to refine the present experimental work. New information, as well as greater accuracy of the results can be obtained. The following steps are suggested.

(1) The visible spectra obtained for the colored samples are of marginal value for comparative purposes, because the apparatus used for the preparation of the various complexes was not feasible for fitting within the sample compartment of the Cary 14 spectrophotometer. It would be valuable if the optical arrangement of the Cary 14 source could be modified so that the beam could be brought out to enable it to pass through the optical windows of the cell. The spectral region is thus extended from infrared, near infrared to the ultraviolet. More spectral features could be observable, such as $h\nu_{CT}$ (possibly in UV region), and absorption edge (possibly in near infrared). More internal electronic transitions could also be observed. Then, comparison of the data between the solid state and solution would allow one to gain more insight about the solid state electronic energy levels. Theoretical work could then be compared in a more quantitative manner.

Figure 19 is a sketch of the possible optical arrangement designed for this purpose. P_1, P_2, P_2', P_1' are four total reflection prisms l_1 and l_2 are condensing lenses, S is sample holder.

(2) Preparation technique: Control of the molecular beam densities is one of the important factors which permits one to obtain pure, uniform samples with proper thickness. Anderson (1) has given a comprehensive description regarding how to control the co-condensation. An effective way to stop both organic and alkali-metal vapor from further deposition after the heaters are turned off is considered to be the most important factor which governs the quantitative complexation between DA

pairs, and the uniformity of the sample as well. The optical and electrical parameters obtained in this way may be more reliable.

The observation of the cation effects using different alkali and alkaline earth metals are suggested for more detailed comparisons. For example, ion association, vibronic effects, polarization and bonding, etc., will be of interest.

(3) Conductivity as well as various optical observations at lower temperatures (below liquid nitrogen temperature) are proposed in order to investigate the possible unusual electrical and optical properties produced by varying the metal-organic ratios. Particularly for the two extreme cases, i.e., either very high concentration of metal or vice versa. One does observe several unusual spectral features in the infrared region, such as described in the next section, when metal concentration is considerably higher than the organic.

(4) It is interesting and valuable to investigate the far infrared spectra of these systems, the DAD, DA or ADA interactions can be estimated from far infrared assignments so as to note trends in charge-transfer forces. These intermolecular vibrations have been reported by Person et al. for pyridine-iodine complex (73) and by Larkindale et al. for TCNE-mesitylene complex (74).

Unusual Results

There are several unusual effects which have been observed in the spectroscopic investigations; first, the emission spectra of the naphthacene impurities in the anthracene crystals, second, naphthalene crystals when doped with potassium atoms gave strong emission bands in the visible region, third, opacity in the infrared from alkali metal aggregates in anthracene crystals. The first two experimental facts have been qualitatively discussed in some detail in this chapter. The last spectral feature was observed in the early stage of the experimental

work. At that time the sample was co-condensed on irtran 6 (hot pressed Cd-Te) as the substrate at liquid nitrogen temperature. The observed unusual features are (a) the very intense absorption from 350 cm^{-1} to 1000 cm^{-1} with no individual infrared bands detected when the metal concentration with high, (b) a strong absorption band around 670 cm^{-1} was obtained in potassium-anthracene co-deposition along with a characteristic weak absorption band of the neutral anthracene (737 cm^{-1}) The spectrum became transparent from 1000 to 1800 cm^{-1} and then opaque at higher frequencies. No vibrational bands of anthracene could be observed beyond 900 cm^{-1}. The concentration of the organic molecules in this case must be larger than in case (a), because the neutral anthracene was detected. The observed spectra are clearly different from the spectrum of pure potassium deposits for which no band could be detected in the infrared region, but only a gradual loss of transmission upon further deposition of pure potassium,

Thin films of solid inert gases containing low concentrations of alkali metal atoms have been studied by esr (68,69) and in optical absorption (68,69,70,71) by a number of investigators. The visible absorption spectrum of sodium atoms in solid benzene has been reported by Duley (72). No infrared data can be found.

It has been indicated by Meyer (70) that potassium-noble gas (Xe, Kr, Ar, and Ne) mixtures are almost always blue and the visible part of the spectrum is strongly concentration dependent; for alkali concentrations smaller than 0.5% no discrete absorption feature is observed. The color is also temperature dependent, because the color of the film will disappear when the temperature of the substrate is increased, a sharp transition point is reached, and the deep film color disappears before

the matrix material vaporizes, leaving a colorless and transparent film. When the temperature of the substrate is brought to room temperature, even thick and concentrated alkali films leave only a thin transparent film. These observations agree very well with the visual results for the very rich potassium samples in our early experiments.

BIBLIOGRAPHY

(1) Günther, Karl-Georg, The Use of Thin Films in Physical Investiga-
     tion. Ed. Anderson (Academic Press, London and New York,
     1966) p. 213.

(2) Li, P. C., J. Paul Devlin, J. Phys. Chem., $\underline{76}$, 1026 (1972).

(3) Schlenk and Bergman, Ann. $\underline{463}$, 84 (1928).

(4) Scott, M. P., J. F. Walker and V. L. Hansly, J. Amer. Chem. Soc.,
     $\underline{58}$, 2442 (1963).

(5) Lipkin, D., D. E. Paul, J. Townsend and S. I. Weissman, Science,
     $\underline{117}$, 534 (1953).

(6) Paul, D. E., D. Lipkin and S. I. Weissman, J. Amer. Chem. Soc.,
     $\underline{78}$, 119 (1956).

(7) DeBoer, E. and S. I. Weissman, Rec. trav. chim. $\underline{76}$, 824 (1957).

(8) Balk, P., G. J. Hoitink and J. W. Schreurs, Rec. trav. chim. $\underline{76}$,
     813 (1957).

(9) Balk, P., S. D. Bruijn and G. J. Hoitink, ibid., $\underline{76}$, 860, 907
     (1957); Hoitink, G. J, ibid., $\underline{76}$, 869, 885 (1957).

(10) Hoitink, G. J., N. H. Velthorst and P. J. Zandstra, Mol. Phys. $\underline{3}$,
     533 (1960).

(11) Slobodyanik, V. V., and A. N. Faidysh, Zh. Fiz Khimii, 257 (1968).

(12) Holmes-Walker, W. A. and A. R. Ubbelohde, J. Chem. Soc. 720 (1954).

(13) Gracey, J. P. V. and A. R. Ubbelohde, ibid., 4080 (1955).

(14) Slough, W. and A. R. Ubbelohde, J. Chem. Soc. 911, 918, 982 (1957).

(15) Martin, G. C. and A. R. Ubbelohde, ibid., 4948 (1961).

(16) Martin, G. C., N. D. Parkyns and A. R. Ubbelohde, ibid., 4958
     (1961).

(17) Suhrman, R., Z. Phys. $\underline{94}$, 742 (1935); $\underline{111}$, 18 (1937).

(18) Inokuchi, H. and Y. Harda, Nature, $\underline{198}$, 477 (1963).

(19) Kearns, D. R. and Calvi, J. Chem. Phys. 34, 2026 (1961).

(20) Marchetti, A. and D. R. Kearns, J. Chem. Soc. 1301 (1966).

(21) Baessler, H., N. Riehl and G. Vaubel, Org. Solid State Chem., Ed.
      George Adler (1969) p. 248.

(22) Eargle and Cox, The Alkali Metals, International Symposium, 116,
      The Chem. Soc. (1967).

(23) Buschow, K. H. J., J. Dielmann, and G. J. Hoijtink, J. Chem. Phys.
      42, 1993 (1965).

(24) Rose, J., Molecular Complexes (Pergamon Press, Oxford, 1967).

(25) Mulliken, R. S., J. Chim. Phys. 61, 20 (1964).

(26) Hall, B. and J. Paul Devlin, J. Phys. Chem. 71, 465 (1967).

(27) Stanley, J., D. Smith, B. Latimer and J. Paul Devlin, J. Phys.
      Chem. 70, (1966).

(28) Moore, J. C., D. Smith, Y. Youhne, and J. Paul Devlin, J. Phys.
      Chem. 75, 325 (1971).

(29) Matsunnaga, Y., J. Chem. Phys. 41, 1609 (1964).

(30) Tamres, M. and J. M. Goodenow, J. Phys. Chem. 71 (7) 1982 (1962).

(31) Merriefield, R. E. and W. D. Phillips, J. Phys. Chem. 80, 2778
      (1958).

(32) Collin, J. and L. D'or, J. Chem. Phys. 23, 397 (1955).

(33) Ferguson, E. E., J. Chim. Phys. 61, 257 (1964).

(34) Ferguson, E. E., and F. A. Matsen, J. Amer. Chem. Soc. 82, 3268
      (1960).

(35) Inokuchi, H. and A. Akamatsu, Solid State Phys. 12, 93 (1961).

(36) Eley, D. D. and G. D. Parfitt, Trans. Faraday Soc., 511, 1529
      (1955).

(37) Friedrich, H. B. and W. B. Person, J. Chem. Phys. 44, 2161 (1966).

(38) Mulliken, R. S., J. Amer. Chem. Soc. 74, 811 (1952).

(39) Nishiguchi, H., Y. Nakai, K. Nakamura, K. Ishizu, Y. Deguchi and
      Takaki, Bull. Chem. Soc. Japan, 38, 185 (1965).

(40) Hush, N. S. and J. R. Rowland, Molecular Phys. 6, 201 (1963).

(41) Briegleb, G., J. Trencseni and W. Herre, Chem. Phys. Letters, 3, 146 (1969).

(42) Mulliken, R. S. and W. B. Person, *Molecular Complexes*, Interscience (1969).

(43) Scherer, J. R., J. Chem. Phys. 36, 3308 (1962).

(44) Gordy, W., J. Chem. Phys. 14, 305 (1946).

(45) Jones, W. D., J. Mol. Spectros. 22, 206 (1967).

(46) Jones, W. D. and V. Hymowitz, ibid., 233 20 (1967).

(47) Behringer, J., In "Raman Spectroscopy", H. Szymanski, Ed., Plenum Press, New York, N. Y. (1967).

(48) Shorygin, P. P., Pure Appl. Chem. 4, 87 (1962).

(49) Kuroda, H., Y. Yoshiihara, and H. Akamatu, Bull. Chem. Soc., Japan 35, 1604 (1962).

(50) Eley, D. D., G. D. Parfitt, M. J. Perry, and D. H. Taysum, Trans. Faraday Soc. 49, 79 (1953).

(51) Eley, D. D. and M. R. Willis, Symposium on Electrical Conductivity in Organic Solids, Ed. H. Kallmann and M. Silver, Interscience, New York, 1961, p. 257.

(52) Eley, D. D., G. D. Parfitt, Trans. Faraday Soc. 51, 1529 (1955).

(53) Eley, D. D., H. Inokuchi and Willis, Discussions Faraday Soc. 28, 54 (1959).

(54) Harding, T. T. and S. C. Wallwork, Acta Cryst., 8, 787 (1955).

(55) Valdes, L. B., Proc. IEE, 42, 420 (1954).

(56) Uchida, T. and H. Akamatu, Bull. Chem. Soc. Japan, 35, 981 (1962).

(57) Buschow, K. H. J. and G. J. Hoijtink, J. Chem. Phys. 40, 2501 (1964).

(58) Katul, J. A. and A. B. Zahlan, J. Chem. Phys. 47, 1012 (1967).

(59) Gorshkove, V. K. and N. D. Zehvandrov, Zhurnal Prikladnoi Spectrskopii, 6, 267 (1967).

(60) Astier, R. and Y. H. Meyer, Chem. Phys. Letters, 11, 523 (1971).

(61) Lippincott, E. R. and E. J. O'Reilly, Jr., J. Chem. Phys. 23, 238 (1955).

(62) Kainer, H. and W. Otting, Chem. Ber. 88, 1921 (1955).

(63) Kiefer, W. and H. Bernstein, Chem. Phys. Letters, 16, 5 (1972).

(64) Kaya, K., N. Mikami, Y. Udagawa and M. Ito, Chem. Phys. Letters, 16, 151 (1972).

(65) Nafie, L. A., P. Stein, and W. L. Peticolas, Chem. Phys. Letters, 12, 131 (1971).

(66) Jen, C. K., V. A. Bowers, E. L. Corchran and S. N. Foner, Phys. Rev. 126, 1749 (1962).

(67) Goldsborough, J. P. and T. R. Koehler, Phys. Rev. 133, A 135 (1964).

(68) McCarty, M. and G. W. Robinson, Mol. Phys. 2, 415 (1959).

(69) Weyhmann, W. and F. M. Pipkin, Phys. Rev. 137, A 490 (1965).

(70) Meyer, B., J. Chem. Phys. 432 986 (1965),

(71) Andrews, L. and G. C. Pimmentel, J. Chem. Phys. 472, 905 (1967).

(72) Duley, W. W., Phys. Letter 27A, 206 (1969).

(73) Yagi, Y., A. I. Popov and W. B. Person, J. Phys. Chem. 71, 2439 (1967).

(74) Larkindale, J. P. and D. J. Simkin, J. Chem. Phys. 563, 730 (1972).

(75) Ferguson, E. E. and F. A. Matsen, J. Chem. Phys. 29, 105 (1958).

(76) Ferguson, E. E. and F. A. Matsen, L. Amer. Chem. Soc. 82, 3268 (1960).

(77) Friedrich, H. B. and W. B. Person, J. Chem. Phys. 44, 2161 (1966).

(78) Balk, P., S. DeBruijn and G. J. Hoijtink Recueil 76, (1957).

(79) Buschow, K. H. J., J. Dieleman and G. J. Hoijtink, J. Chem. Phys. 42, 1993 (1965).

(80) Lipkin, D., D. E. Paul, J. Townsend and S. I. Weissman, J. Am. Chem. Soc. 78, 119 (1956).

(81) See, for example, a) Gracey, J. P. V. and A. R. Ubbelohde, J. Chem. Soc. 4089 (1955); and b) Martin, G. C., N. D. Parkyns and A. R. Ubbelohde, J. Chem. Soc. 4958 (1961).

(82) Slobodyanik, V. V. and A. N. Faidysk, Opt. Spektrosk 26, 138 (1969).

(83) Valdes, L. B., Proc. I. R. E., 41, 420 (1954).

(84) Stanley, J. D. Smith, B. Latimer and J. P. Devlin, J. Phys. Chem. 70, 2011 (1966).

(85) See, for example, Andrews, L., J. Chem. Phys. 54, 4935 (1971).

(86) Levin, I., Spectrochim. Acta 25A, 1157 (1969).

(87) Matsunaga, Y., J. Chem. Phys. 42, 1982 (1965).

(88) See, for example, Mulder, B. J., J. Phys. Chem. Solids 29, 182 (1968).

(89) Behringer, J., In "Raman Spectroscopy", H. Szymanski, Ed., Plenum Press, New York (1967).

(90) Califano, S., J. Chem. Phys. 36, 903 (1962).

(91) Abasbegovic, N., N. Vukotic and L. Colombo, J. Chem. Phys. 41, 2575 (1964).

(92) Suzuki, M., T. Yokoyama and M. Ito, Spectrochim. Acta 24A, 1091 (1968).

(93) Gutman, F. and L. E. Lyons, Organic Semiconductor (1967) p. 465.

(94) LeBlanc, Jr., J. Chem. Phys. 42, 4307 (1965).

APPENDIX

SOLID STATE SPECTRA AND CONDUCTIVITIES OF

THE POTASSIUM SALTS OF ANTHRACENE

Crossed molecular beam vapor cocondensation techniques have been
used to prepare thin films of the potassium salts of anthracene in a
form well suited to both infrared and Raman sampling. Three distinct
stoichiometric salts, as contrasted to solid solutions of potassium in
antrhracene, are apparently produced by variation of the metal-anthra-
cene ratio. Though the existence of distinct salt crystals is strongly
suggested by the observation of three sets of characteristic infrared
and Raman bands, an identification of the salts as KA_2, KA and K_2A re-
mains tentative. The vibrational data represent the best available
empirical evidence of the effect of electron transfer on the bond
strengths in anthracene but are of marginal value barring transformation
into force constants. Resistivities and electronic absorption spectra
have also been measured for selected samples. Resistivity values, which
roughly match those reported by Ubbelohde, decreased somewhat with in-
creasing metal to organic deposition ratios. The anthracene skeletal
symmetric stretching mode gave a strong resonance Raman effect with 5145
A (green) excitation of the K_2A salt.

Introduction

The polycyclic hydrocarbon anions, typified by the mono- and dineg-

88

ative ions of anthracene, are of interest as possible reaction intermediates, as subjects for the testing of chemical bonding theories and because their solid state salts may be characterized by unusual electrical properties. Thus, Hoijtink et al., have argued that one electron L.C.A.O.M.O. methods apply more quantitatively to the mono- and dinegative ions than to the corresponding neutral arenes (78) and have compared theoretical predictions with liquid solution transition energies (79). The radical anion esr spectra have long been of interest (80) primarily as information regarding charge densities and the association with cations in solutions. However, solid state studies have been almost completely restricted to the work by Ubbelohde et al., on dielectric and conductivity properties of bulk solids with alkali metal donors (81). The bulk solids were not characterized by either x-ray or spectroscopic methods but were apparently viewed as solid solutions of alkali metals in the crystalline arenes.

Although the bond order changes that accompany electron transfer to various arenes have been estimated theoretically (78), no direct experimental measure of the differences in bonding between the arene anions and the parent hydrocarbons have been reported. In particular, neither solution nor solid state vibrational spectra are available. Solid state fluorescent spectra for alkali metal-anthracene salts of unknown composition have been described (82) but electronic spectra for stoichiometric solid salts are apparently missing from the literature.

A basically spectroscopic study of the potassium salts of anthracene is reported here as part of a more general study to obtain solid state vibrational and electronic spectra for stoichiometric salts of arene anions. Such data will allow ready identification of these salts

in the future and, also, permit the determination of empirical force constants for certain arene anions and, thus, a comparison with theoretical predictions of bond order changes relative to the neutral arenes. Finally, resistivities determined by the four point probe method (83) on thin salt films will be compared with values reported by Ubbelohde for related bulk samples (81).

Experimental

The potassium salts of anthracene have been prepared by cocondensation of the metal with the organic from molecular beams which cross at the surface of a substrate having properties appropriate for the anticipated measurement. The techniques are an extension of those originally developed for infrared sampling of thin films of the alkali metal salts of tetracyanoethylene (84). The molecular beams originated from Knudsen cells containing the liquid metal ($\sim 200^{\circ}$C) and crystalline anthracene ($\sim 120^{\circ}$C). The Knudsen cells were mounted within the vacuum shroud of a low temperature cell (resembling those commonly employed in matrix isolation spectroscopy) (85) and directed towards the cyrotip which supported appropriate substrates for absorption, Raman scattering and conductivity measurements. Deposition was thus simultaneously onto a central CsBr optical plate, an aluminum wedge for Raman sampling by the single reflection technique (86) and a gold striped fused quartz plate for conductivity measurements. The ratio of metal to organic in the condensate was controlled by varying the Knudsen cell temperatures.

Originally depositions were made at $\sim 100^{\circ}$K (substrate temperature) but the occlusion of unreacted potassium or anthracene aggregates, though a source of some unusual spectroscopic effects, tended to confuse

both the spectroscopic and conductivity results. Consequently, the technique has evolved wherein the thin films are prepared at 25° C but subsequently cooled to liquid N_2 temperatures for most measurements. The reduced temperatures kinetically stabilized the deposits which detectably deteriorate in a few hours at 25° C, even in a 10^{-5} torr vacuum. Since the anthracene is volatile at 25° C, the warmer temperatures guarded against deposition of pure anthracene in anthracene rich deposits while the potassium was sufficiently mobile at 25° C to insure the absence of metal aggregates in a 2:1 (metal rich) deposit. The warmer substrate temperatures did necessitate that more extreme precautions be taken to eliminate surface moisture, since, at 25° C, such moisture is highly reactive towards the anthracene salts.

The deposits were transparent, brightly colored (yellow-green through blue) films a few microns thick as required for measurement of the infrared spectra. Raman spectra were also easily obtained, although sample fluorescence (probably from tetracene impurity in most cases) often dictated a choice of the laser excitation wavelength of 5145 Å rather than 4880 Å. The sample film thicknesses, optimized for measurement of vibrational spectra, were, in general, too great for observation of details in the electronic absorption spectra though qualitative data have been obtained.

Infrared data were recorded from 600 to 4,000 cm^{-1} on a Beckman IR-7 spectrometer, while the Raman and visible absorption measurements were with a Jarrell-Ash 25-100 dual monochromator fitted with an ITT FW-130 PM tube and photon counting gear. Raman spectra were excited with a Coherent Radiation Model 52 argon ion laser using both the 4880 Å (blue) and 5145 Å (green) lines. The electronic spectra were determined in a

single beam mode with a tungsten lamp source and using the Jarrell-Ash system, rather than a conventional uv-visible instrument, as dictated by the size and geometry of our sampling system. Resistivities were deduced from voltage and current measurements from the thin films on a fused quartz substrate using a four-point probe (83). Current measurements were with a Keithley Model 417 picoammeter while voltages were followed using a Philbrick/Nexus millivoltmeter.

Results and Discussion

Vibrational Spectra

Both the vibrational and electronic spectra of the codeposits clearly suggest that the anthracene molecule can assume three distinctly different forms in the potassium – anthracene solid films. Each form has a unique vibrational spectrum that differs significantly from that of pure anthracene and, thus, suggests that considerable ionic character is involved in the metal-organic interaction in each case (87). Based on the approximate K:A ratios that produce the films in which the various unique spectra are dominant, it is suggested that the different anthracene forms correspond to a) two anthracene molecules with one associated potassium atom (KA_2), b) one anthracene molecule per associated potassium atom (KA), c) one anthracene molecule per two associated potassium atoms (K_2A).

Although it has been possible to obtain KA and K_2A in nearly pure form, this alone does not completely confirm that stoichiometric salt crystals of regular structure are the dominant solid forms. It is still conceivable that the solids are basically solutions of continuously variable composition with irregular structures in which KA_2, KA and K_2A
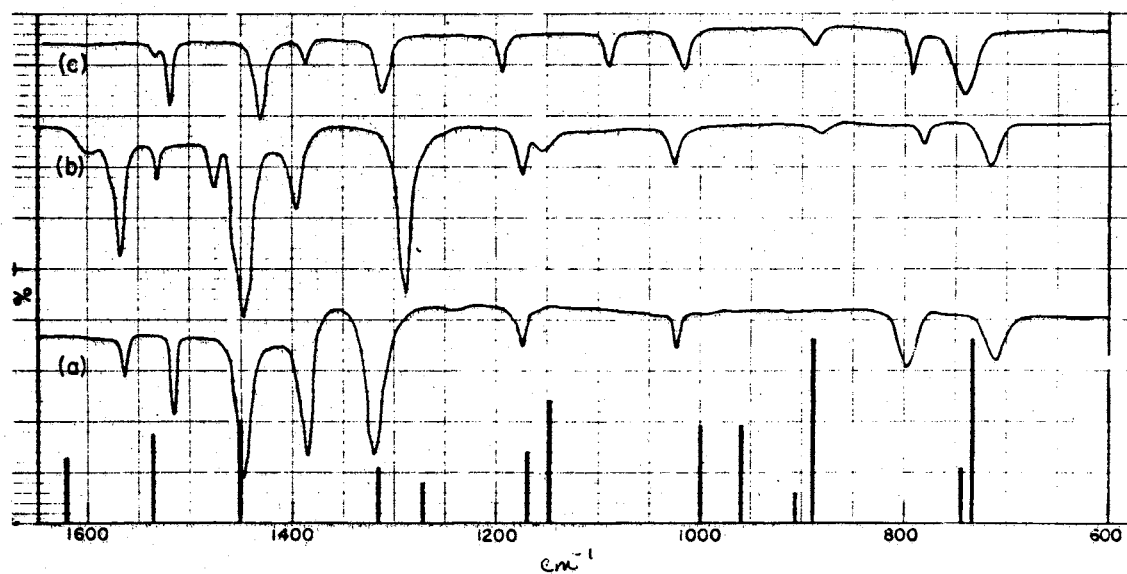
Figure 20. Infrared Spectra for Anthracene (Bar Graph) and Potassium
Slats of Anthracene: a) KA$_2$, b) KA and c) K$_2$A
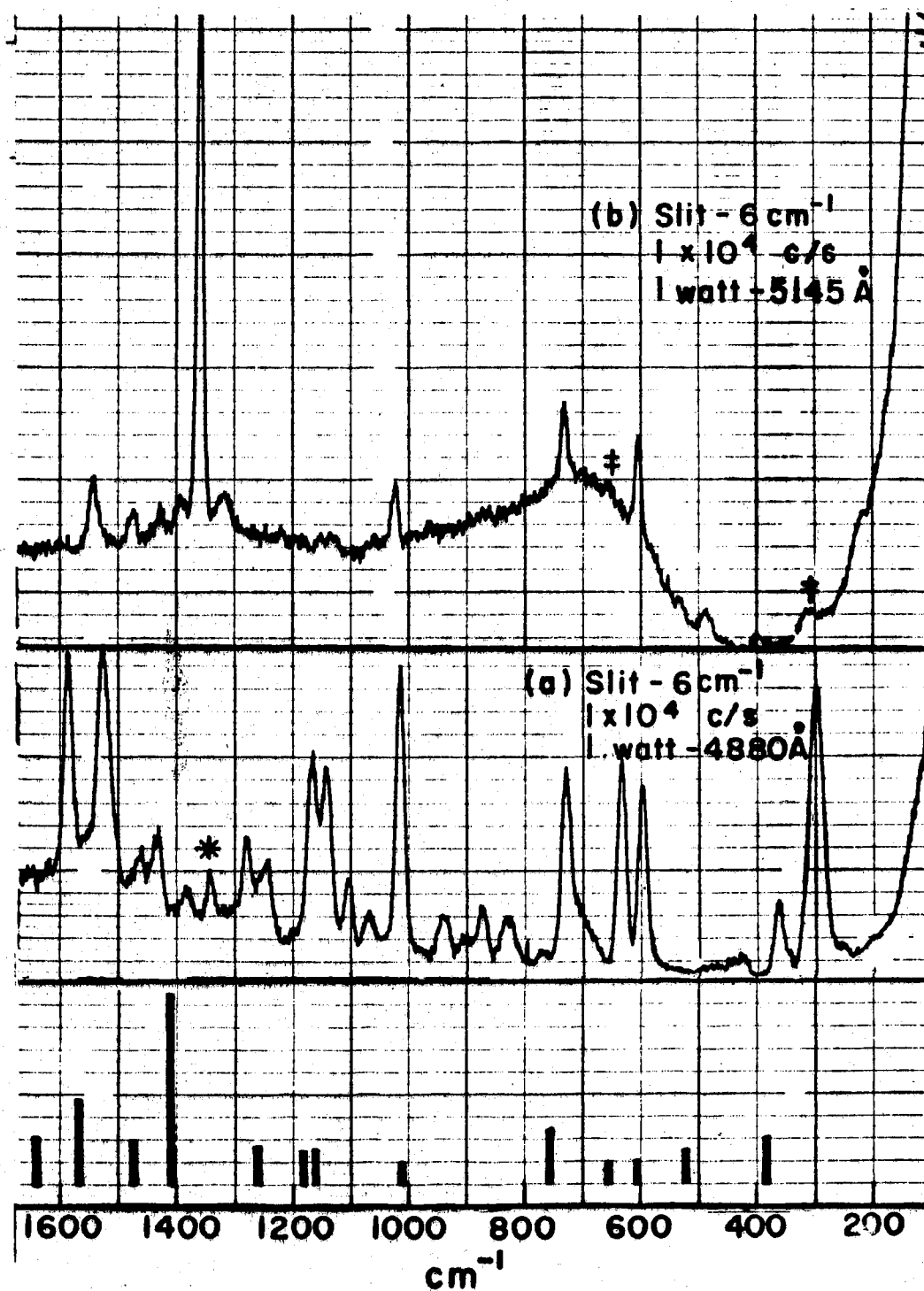
Figure 21. Raman Spectra for Anthracene (Bar Graph) and Potassium
Salts of Anthracene: a) K_2A and b) KA

units occur with a frequency dictated by the metal-organic ratio deposited. However, it is our judgement that the uniqueness and sharp quality of the three sets of vibrational spectral features are indicative of the formation of three regular stoichiometric salts, KA_2, KA and K_2A, with the potassium assuming a cationic form in each case. Tentatively, and as a basis for discussing the various experimental results, we have assumed that three salts are formed: yellow-green KA_2, green KA and green-blue K_2A.

The infrared spectra for the three salts and the Raman spectra for K_2A and KA, along with the spectra for pure anthracene, are presented in Figures 20 and 21. The Raman spectra are untouched while the infrared curves are composites of measurements from several different deposits. No Raman spectrum for KA_2 is shown although a few band frequencies are listed in Table I. This reflects the instability of this salt, particularly in the laser beam, which prevented its preparation in a form approaching the pure state.

The untouched Raman curves of Figure 20 are evidence of the near purity of certain of the K_2A and KA films. It should be emphasized, however, that the preparation procedures only guarantee that the "K_2A" deposits are richer in K than the "KA" deposits but do not require that the actual metal to organic ratios be 2:1 and 1:1, respectively. In other words, despite the control of such parameters as temperature and orifice size, the relative densities of the molecular beams from the potassium and anthracene Knudsen cells have not been established with sufficient accuracy. What is known is that the bands in Figure 20a (or 20b) go with a single compound judging from their constant relative intensities over the range of deposition ratios in which they are detect-

able. The stability of the mono- and dinegative anthracene anions in solution (79) favor the KA and K_2A choice for the stable salts.

The vibrational data for the three salts are tabulated in Tables XI and XII with an attempt made to follow the frequency variation of some modes through the series $A \rightarrow K_2A$. It is expected that a force constant analysis will establish more clearly the trends in bond order changes for this series and eventually permit reliable assignments of the vibrational data to molecular normal modes. Until such empirical force constants have been determined (from a study now in progress) the precise significance of the individual frequency shifts will remain obscure. It can be noted, however, that theory predicts that certain bonds will be strengthened while others are weakened as a result of one and two electron transfer to anthracene (78). Thus, although the transferred electron (s) has a net antibonding quality, an orderly decrease in the fundamental frequencies is not expected. In fact, irregularities are apparent in the behavior of certain modal frequencies in Tables XI and XII (e.g., the anthracene mode at 1009 cm^{-1} increases to 1022 cm^{-1} in KA but then decreases to 1017 in K_2A). The lack of a completely regular pattern makes a force constant analysis an imperative step in any quantitative consideration of bonding effects.

Electronic Absorption Spectra

Qualitatively useful visible absorption spectra for the anthracene salts are presented in Figure 3 for the frequency range 12 to 21 kK; the region where new bands are known to appear in the solution spectra of these anions. The electronic spectra are of particular interest for comparison with solution spectra reported for the mono- and dianions
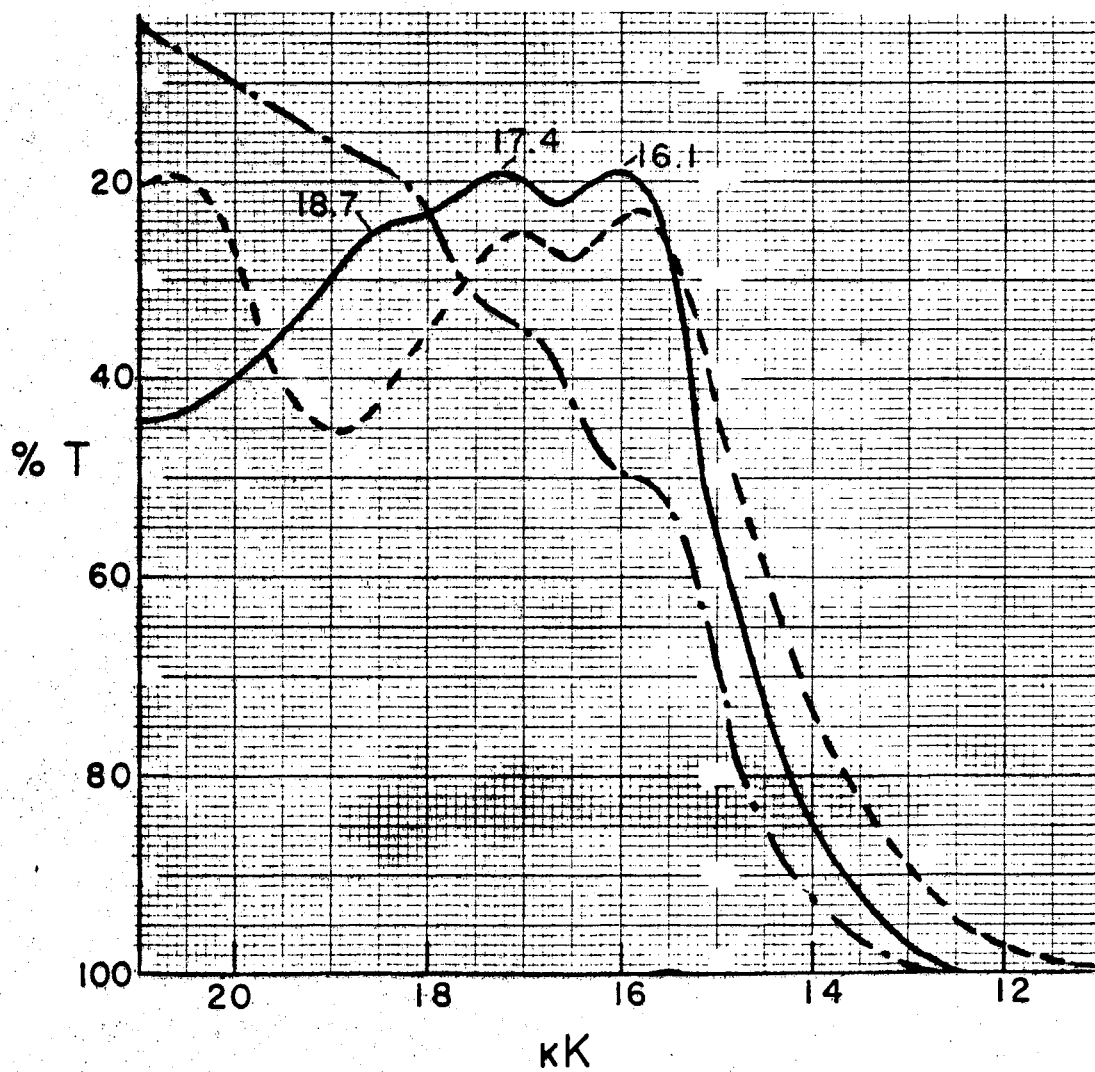
Figure 22. Electronic Absorption for K_2A; KA and KA_2

TABLE XI

FREQUENCIES (CM^{-1}) FOR INFRARED BANDS OF ANTHRACENE, KA_2, KA AND K_2A[b]

Anthracene[a]	KA_2	KA	K_2A
3049	----	3030	3010
3022	----	2990	2960
		1600	
1620	1564	1567	1533
		1530	
1533	1515	1475	1519
1448	1448	1445	1431
1398	1383	1395	1387
1316	1320	1288	1312
1269	----	----	----
1169 } 1150	1173	1175	{ 1194 1155
			1090
999	1023	1025	1016
956	----	----	----
886	----	882	888
743	798	782	793
737 } 727	710	715	740

[a]From reference 90; only the stronger anthracene features are listed here.

[b]For relative intensities, see Figure 20.

TABLE XII

FREQUENCIES (CM^{-1}) OF RAMAN BANDS OF ANTHRACENE, KA_2, KA AND K_2A^c

Anthracene[a]	KA_2	KA	K_2A
			2715
1632		1598	1542
1555		1538	1470
1481	1471	1442	1390
1403		1395	1357
		1293	1315
1261	1260	1260	
1188		1180	1160
1165	1155	1152	
1009	1025	1022	1017
956[b]		950	
904[b]	~900	880	
		835	
754	738	735	722
655		642	650(?)
602		605	595
525			480
395		370	390
290[b]		305	210(?)

[a]From reference 91.

[b]From reference 92.

[c]For relative intensities, see Figure 21.

associated with various cations (79). The visible spectra were also of interest in this study because resonance Raman effects have been detected (see next section) that suggest absorption patterns requiring substantiation.

The salt spectra resemble those of the corresponding solvated anion. Thus, K_2A has a structured absorption band centered near 18 kK as does the dianion in association with the potassium cation in solution (79). The comparison for the KA salt with the mononegative anion spectrum shows a greater difference, but the red shift relative to K_2A is in the direction of the ~14 kK band peak reported for the mononegative anion associated with Na^+ in solution (79). The absorption curve for the KA_2 solid, like most of the data for this extremely unstable compound, may be less reliable. The KA_2 spectrum, however, is markedly different than for the other salts with no obvious band maxima in the 12 to 21 kK range, a fact consistent with the yellow-green color.

The K_2A absorption band system near 18 kK has components spaced by ~1300 cm^{-1} with maxima at 16.1, 17.4, and 18.7 kK. The spacing of maxima is reminiscent of that of ~1400 cm^{-1} in the familiar absorption and fluorescence spectra of pure anthracene (88) and suggests that the same vibrational mode, a symmetric ring stretching mode, is involved in the dianion absorption process.

K_2A Resonance Raman Effect

The colored quality of the salts and the nature of the Raman sampling procedure favored observation of the resonance Raman phenomenon (89). In particular, the visible absorption spectrum for the K_2A salt (Figure 22) indicates that the 18.7 kK component is absorbing at the 19.4 kK fre-

quency of the argon laser green line. Further, the thin film character of the samples minimized the probability of reabsorption of resonantly scattered light. Thus, not surprisingly, the K_2A Raman active mode at 1357 cm^{-1} gave a strong Resonance Raman effect with green line (5145Å) excitation. This mode displayed a normal intensity with blue (4880Å) excitation, but appeared with a factor of five greater intensity than any other K_2A Raman feature when the 5145Å line was used. It is possible that other modes displayed less pronounced resonance scattering, but only the intensity of the K_2A feature at 1357 cm^{-1} varied in a striking manner with change of excitation frequency. The resonant character of the scattering was further evidenced by a significant overtone intensity (2715 cm^{-1}).

As was noted above, the K_2A electronic absorption (~18 kK) was characterized by components spaced by ~1300 cm^{-1}. This observation is undoubtedly relevant to the resonant scattering noted for the 1357 cm^{-1} mode since it is known that the resonance effect is most pronounced when the excitation frequency is matched to a vibronic absorption feature involving the vibrational mode in question (89). In other words, the resonant scattering at 1357 cm^{-1} is consistent with the assignment of the structure on the electronic absorption band as the result of vibronic transitions involving the anthracene ring symmetric stretching mode. Of course, the ~1300 cm^{-1} value would be characteristic of the mode for the electronic excited state.

Conductivity Results

Ubbelohde, et al. have described rather extensive studies of the electrical characteristics of the alkali metal - anthracene crystals

prepared from solution. They conclude that the conductivity increases significantly as the metal to anthracene ratio is increased, but that resistivities remain quite high--in the 10^8-10^{10} ohm-cm range at 20°C. Though our thin film spectroscopic results seem to contradict their view of the solids as solutions of metal atoms in anthracene with a continuously variable composition, the new data support their contention that electron transfer occurs from the metal atoms to anthracene. Further, our resistivity data, obtained by the four-point probe method, are reasonably compatible with the published values from the bulk samples. Thus, the resistivity was observed to decrease roughly two decades as the metal to anthracene ratio was varied from 1:2 to 2:1. However, the measured thin film resistivities were significantly lower than those reported for bulk samples of comparable composition, the range extending from 10^6 to 10^8 ohm-cm at ~100°K. Our data do not warrant a more quantitative presentation at this time.

Acknowledgements

VITA

Paul Ching Li

Candidate for the Degree of

Doctor of Philosophy

Thesis: SPECTROSCOPIC PROPERTIES AND RESISTIVITIES OF SOME ALKALI METAL-
ARENE CHARGE-TRANSFER COMPLEXES

Major Field: Chemistry

Biographical:

Personal Data: Born in Kiang-su, China, November 7, 1939, the son
of Chai-cheh and I-wen Li.

Education: Graduated from Subordinate High School of Taiwan Pro-
vincial Normal University in Taipei, Taiwan, China in 1955;
received the Bachelor of Science degree with a major in Agri-
cultural Education from Taiwan Provincial Chung-hsing Univer-
sity in July 1959; completed the requirements for the Doctor
of Philosophy degree in May 1973.

Professional Experience: Graduate Research Assistant, Oklahoma
State University 1967 to 1973. Factory Chemist in Swan Rubber,
Division of Emerace Esna since May 1971.